Supporting Information

Combination of a New Chiroptical Probe and Theoretical Calculations for Chirality Detection of Primary Amines

Shunsuke Kuwahara,* Masaya Nakamura, Akira Yamaguchi, Mari Ikeda, and Yoichi Habata

Department of Chemistry, Faculty of Science, Toho University, 2-2-1 Miyama, Funabashi, Chiba 274-8510, Japan

Materials and methods

All reagents and solvents were commercially available and used without further purification. IR spectra were obtained as KBr disks on a JASCO FT/IR-410 spectrophotometer. ^{1}H-NMR spectra were recorded on Jeol ECP400 (400 MHz) spectrometers. ^{13}C NMR spectra were obtained on Jeol ECP400 (100 MHz) spectrometers. All NMR spectroscopic data of $CDCl_3$ solutions are reported in ppm (δ) downfield from TMS. UV and CD spectra were recorded on JASCO V-650 and JASCO J-820 spectrometers, respectively. CD spectra were recorded with the following measurement parameters: scan speed, 20 nm/min; resolution, 0.2 nm; bandwidth, 1.0 nm; response, 4.0 s; 4−10 accumulations.

Silica gel 60 F254 precoated plates on glass from Merck Ltd. were used for thin layer chromatography (TLC).

Synthesis of chiroptical probe 1

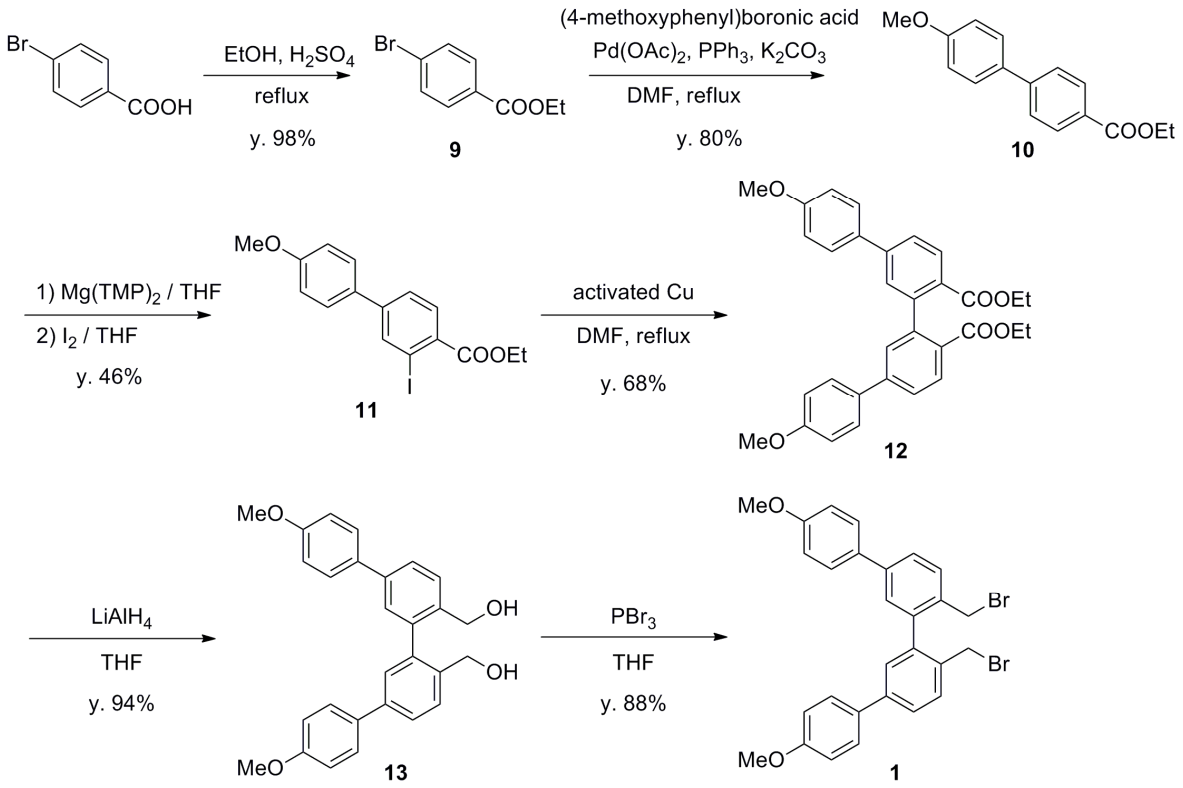

Ethyl 2-iodine-4-(4-Methoxyphenyl)benzonate (11)

Ethyl 4-(4-Methoxyphenyl)benzonate (**10**)[1] was synthesized by Suzuki-Miyaura coupling from ester **9**. Iodination of **10** was carried out according to the literature procedure.[2] To a THF solution of $(TMP)_2Mg$ (0.29 M, 22 mmol) was added **10** (0.95 g, 3.7 mmol) in dry THF (10 mL) dropwise at 0 °C under N_2 atmosphere and the mixture was stirred at room temperature for 3.5 h. After being cooled to –78 °C, a THF (10 mL) solution of I_2 (5.6 g, 22 mmol) was added and stirring was continued for 1 h at room temperature. The mixture was then poured into cooled 1 N HCl, washed with saturated Na_2SO_3, and extracted with $CHCl_3$. The organic layer was dried over Na_2SO_4 and evaporated to dryness. The

crude product was purified by column chromatography on silica gel ($CHCl_3$ as eluent) to yield ester **11** (0.66 g, 46%) as pale red oil; ^{1}H NMR (400 MHz, $CDCl_3$) δ 8.19 (d, J = 1.8 Hz, 1H), 7.87 (d, J = 8.1 Hz, 1H), 7.57 (dd, J_1 = 8.8 Hz, J_2 = 1.8 Hz, 1H), 7.52 (dd, J_1 = 8.8 Hz, J_2 = 2.1 Hz, 2H), 6.98 (dd, J_1 = 8.8 Hz, J_2 = 2.1 Hz, 2H), 4.40 (q, J = 7.1 Hz, 2H), 3.87 (s, 3H), 1.41 (t, J = 7.1 Hz, 3H); ^{13}C NMR (100 MHz, $CDCl_3$) δ 166.3, 160.1, 145.2, 139.5, 132.7, 131.3, 130.7, 128.4, 125.9, 114.5, 61.6, 55.4, 14.3; *m/z* (matrix: DTT/TG = 1/1) = 383 ($[M+1]^+$, 100%). Because of instability of ester **11**, elemental analysis was not carried out.

Ethyl (2-Ethyl 4-(4-Methoxyphenyl)benzonate)-4-(4-Methoxyphenyl)benzonate (12)

A solution of ester **11** (0.304 g, 0.794 mmol) in dry DMF (1 mL) was added activated Cu (1.28 g, 6.6 mmol) and the mixture was stirred at 135 ^{o}C for 2 days. After cooling to room temperature, the mixture was filtered through a pad of Celite, and then AcOEt was added. After washing with 1 N HCl and brine, the organic layer was dried over Na_2SO_4 and evaporated to dryness. The crude product was purified by column chromatography on silica gel (hexane/EtOAc, v/v 20:1 to 4:1 as eluent) to yield diester **12** (0.14 g, 68%)) as white needles: mp 131.0-131.8 ^{o}C ; ^{1}H NMR (400 MHz, $CDCl_3$) δ 8.09 (d, J = 8.1 Hz, 2H), 7.63 (dd, J_1 = 8.1 Hz, J_2 = 1.9 Hz, 2H), 7.59 (dd, J_1 = 8.8 Hz, J_2 = 2.2 Hz, 4H), 7.45 (d, J = 1.9 Hz, 2H), 6.98 (dd, J_1 = 8.8 Hz, J_2 = 2.2 Hz, 4H), 4.06 (m, 4H), 3.85 (s, 6H), 0.98 (t, J = 7.2 Hz, 6H); ^{13}C NMR (100 MHz, $CDCl_3$) δ 167.1, 159.8, 144.1, 143.6, 132.2, 130.6, 128.4, 128.3, 128.0, 125.0, 114.3, 60.5, 55.4, 13.7; IR (KBr) ν_{max} 3034, 2981, 2937, 2835, 1719, 1599, 1519, 1484, 1280, 1251, 1089, 1044, 893, 828 cm^{-1}; *m/z* (matrix: DTT/TG = 1/1) = 511 ($[M+1]^+$, 25%); Anal. Calcd for $C_{32}H_{30}O_6$: C, 75.28; H, 5.92. Found: C, 75.09; H, 5.87.

(4,4'''-Dimethoxy-1,1':3',1'':3'',1'''-quaterphenyl-4',6''-diyl)dimethanol (13)

To a mixture of $LiAlH_4$ (0.0314 g, 0.826 mmol) and dry THF (1.0 mL) cooled at 0 ^{o}C was added dropwise a solution of diester **12** (0.115 g, 0.226 mmol) in dry THF (2.0 mL), and the reaction mixture was stirred at room temperature for 1.5 h. The reaction mixture was quenched with a minimum amount of water, and the organic layer was filtered. The organic layer was dried over Na_2SO_4 and evaporated to dryness to yield diol **13** (0.14 g, 68%)) as white needles: mp 154.0-155.0 ^{o}C; ^{1}H NMR (400 MHz, $CDCl_3$) δ 7.62 (dd, J_1 = 7.7 Hz, J_2 = 1.6 Hz, 2H), 7.58−7.55 (m, 6H), 7.43 (d, J = 1.6 Hz, 4H), 6.97 (d, J = 8.8 Hz, 2H), 4.47 (m, 4H), 3.85 (s, 6H), 2.57 (s, 2H); ^{13}C NMR (100 MHz, $CDCl_3$) δ 159.4, 140.5, 140.2, 137.1, 132.8, 130.2, 128.2, 126.3, 114.3, 62.7, 55.4; IR (KBr) ν_{max} 3360, 3034, 2999, 2923, 2837, 1609, 1519, 1487, 1248, 1035, 890, 817 cm^{-1}; *m/z* (matrix: DTT/TG = 1/1) = 392 ($[M-2OH]^+$, 20%); Anal. Calcd for $C_{28}H_{26}O_4$: C, 78.85; H, 6.14. Found: C, 78.58; H, 6.10.

4',6''-Bis(bromomethyl)-4,4'''-dimethoxy-1,1':3',1'':3'',1'''-quaterphenyl (1)

PBr_3 (0.1 mL, 1 mmol) was added to a solution of diol **13** (0.085 g, 0.20 mmol) in dry THF (1.2 mL) at 0°C, and the reaction mixture was stirred at room temperature for 1 h. The reaction mixture was quenched with a minimum amount of water, and then AcOEt was added. After washing with 5% aq. $NaHCO_3$ and brine, the organic layer was dried over Na_2SO_4 and evaporated to dryness. The crude product was recrystallized from hexane/EtOAc to yield dibromide **1** (0.097 g, 88%) as white needles: mp 164.0-165.0 °C; ^{1}H NMR (400 MHz, $CDCl_3$) δ 7.64-7.58(m, 8H), 7.55 (s, 2H), 6.98 (d, J = 8.8 Hz, 4H), 4.38 (m, 4H), 3.85 (s, 6H); ^{13}C NMR (100 MHz, $CDCl_3$) δ 159.5, 140.8, 139.9, 134.1, 131.2, 128.3, 128.2, 126.8, 114.3, 55.4, 32.2; IR (KBr) ν_{max} 3057, 3019, 2963, 2935, 2834, 1606, 1517, 1481, 1249, 1177, 1030, 903, 821, 591 cm^{-1}; *m/z* (matrix: DTT/TG = 1/1) = 550 ([M-2]$^+$, 10%), 552 ([M]$^+$, 20%), 554 ([M+2]$^+$, 10%); Anal. Calcd for $C_{28}H_{24}Br_2O_2$: C, 60.89; H, 4.38. Found: C, 60.97; H, 4.41.

Coupling reaction of chiroptical probe 1 with chiral amines

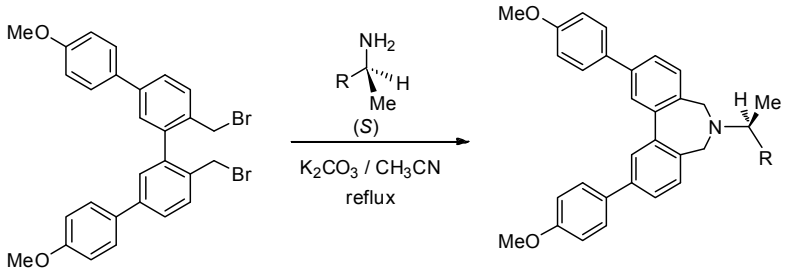

1

(*S*)-**2a** : R = *t*-Bu (y. 95%)
(*S*)-**3a** : R = cyclohexyl (y. 96%)
(*S*)-**4a** : R = *i*-Pr (y. 83%)
(*S*)-**5a** : R = *n*-Bu (y. 85%)
(*S*)-**6a** : R = Et (y. 89%)
(*S*)-**7a** : R = Ph (y. 97%)
(*S*)-**8a** : R = 2-Naph (y. 92%)

6-[(2*S*)-3,3-dimethylbutan-2-yl]-2,10-bis(4-methoxyphenyl)-6,7-dihydro-5*H*-dibenzo[*c*,*e*]azepine ((*S*)-2a)

A mixture of dibromide **1** (12 mg, 0.022 mmol), (*S*)-3,3-dimethylbutan-2-amine (3.00 μL, 0.037 mmol) and K_2CO_3 (8.7 mg, 0.063 mmol) in CH_3CN (0.3 mL) was refluxed for 2 h. After cooling to room temperature, the mixture was filtered through a pad of Celite, and then evaporated to dryness. The crude product was purified by column chromatography on silica gel (EtOAc as eluent) to yield amine (*S*)-**2a** (10.3 mg, 95%) as colorless prisms: mp 155.5 °C (dec.); ^{1}H NMR (400 MHz, $CDCl_3$) δ 7.71 (d, J = 1.8 Hz, 2H), 7.60 (d, J = 8.7 Hz, 4H), 7.55 (dd, J_1 = 7.8 Hz, J_2 = 1.8 Hz, 2H), 7.41 (d, J = 7.8 Hz, 2H), 6.99 (d, J = 8.7 Hz, 4H), 3.86 (s, 6H), 3.68 (d, J = 12.5 Hz, 2H), 3.57 (d, 12.5 Hz, 2H), 2.63 (q, J = 7.0 Hz, 1H), 1.14 (d, J = 7.0 Hz, 3H), 0.99 (s, 9H); ^{13}C NMR (100 MHz, $CDCl_3$) δ 159.2, 141.4, 140.1, 135.7, 133.6, 130.3, 128.2, 126.2, 125.8, 114.3, 68.7, 55.4, 54.5, 36.8, 27.1, 11.6; IR (KBr) ν_{max} 3038, 2995, 2954, 2834, 1608, 1518, 1488, 1284, 1266, 1244, 1046, 892, 821 cm^{-1}; *m/z* (matrix: DTT/TG = 1/1) = 492 ([M+1]$^+$, 60%); Anal. Calcd for $C_{34}H_{37}NO_2$: C, 83.06; H, 7.59; N, 2.85.

Found: C, 83.00; H, 7.33; N, 2.77.

6-[(2*R*)-3,3-dimethylbutan-2-yl]-2,10-bis(4-methoxyphenyl)-6,7-dihydro-5*H*-dibenzo[*c*,*e*]azepine ((*R*)-2a)

Colorless prisms: mp 155.5 °C (dec.); ^{1}H NMR (400 MHz, $CDCl_3$) δ 7.70 (d, *J* = 1.8 Hz, 2H), 7.60 (d, *J* = 8.8 Hz, 4H), 7.55 (dd, J_1 = 7.8 Hz, J_2 = 1.8 Hz, 2H), 7.41 (d, *J* = 7.8 Hz, 2H), 6.99 (d, *J* = 8.8 Hz, 4H), 3.86 (s, 6H), 3.68 (d, *J* = 12.5 Hz, 2H), 3.57 (d, 12.5 Hz, 2H), 2.63 (q, *J* = 7.0 Hz, 1H), 1.14 (d, *J* = 7.0 Hz, 3H), 0.99 (s, 9H); ^{13}C NMR (100 MHz, $CDCl_3$) δ 159.2, 141.4, 140.1, 135.7, 133.6, 130.3, 128.2, 126.2, 125.8, 114.3, 68.7, 55.4, 54.4, 36.8, 27.1, 11.6; IR (KBr) ν_{max} 3022, 2997, 2952, 2833, 1607, 1518, 1489, 1294, 1270, 1037, 889, 821 cm^{-1} ; *m/z* (matrix: DTT/TG = 1/1) = 492 ([M+1]$^+$, 20%); Anal. Calcd for $C_{34}H_{37}NO_2$·1/10AcOEt: C, 82.56; H, 7.61; N, 2.80. Found: C, 82.38; H, 7.54; N, 2.85.

6-[(1*S*)-1-cyclohexylethyl]-2,10-bis(4-methoxyphenyl)-6,7-dihydro-5*H*-dibenzo[*c*,*e*]azepine ((*S*)-3a)

Colorless prisms: mp 157.5 °C (dec.); ^{1}H NMR (400 MHz, $CDCl_3$) δ 7.71 (d, *J* = 1.8 Hz, 2H), 7.60 (d, *J* = 8.8 Hz, 4H), 7.55 (dd, J_1 = 7.7 Hz, J_2 = 1.8 Hz, 2H), 7.42 (d, *J* = 7.7 Hz, 2H), 6.99 (d, *J* = 8.8 Hz, 4H), 3.85 (s, 6H), 3.61 (d, *J* = 12.5 Hz, 2H), 3.53 (d, 12.5 Hz, 2H), 2.55 (quin, *J* = 6.7 Hz, 1H), 1.98-1.59 (m, 5H), 1.29-0.97 (m, 9H); ^{13}C NMR (100 MHz, $CDCl_3$) δ 159.2, 141.5, 140.2, 135.1, 133.5, 130.3, 128.2, 126.1, 125.8, 114.3, 64.0, 55.4, 52.1, 41.6, 31.2, 29.0, 26.9, 26.8, 26.6, 13.8; IR (KBr) ν_{max} 3022, 2997, 2952, 2833, 1607, 1518, 1489, 1294, 1270, 1037, 889, 821 cm^{-1}; *m/z* (matrix: DTT/TG = 1/1) = 519 ([M+2]$^+$, 65%); Anal. Calcd for $C_{36}H_{39}NO_2$: C, 83.52; H, 7.59; N, 2.71. Found: C, 83.34; H, 7.29; N, 2.72.

2,10-bis(4-methoxyphenyl)-6-[(2*S*)-3-methylbutan-2-yl]-6,7-dihydro-5*H*-dibenzo[*c*,*e*]azepine ((*S*)-4a)

Colorless prisms: mp 147.9 °C (dec.); ^{1}H NMR (400 MHz, $CDCl_3$) δ 7.72 (d, *J* = 1.8 Hz, 2H), 7.60 (d, *J* = 8.7 Hz, 4H), 7.55 (dd, J_1 = 7.8 Hz, J_2 = 1.8 Hz ,2H), 7.42 (d, *J* = 7.8 Hz, 2H), 6.99 (d, *J* = 8.7 Hz, 4H), 3.86 (s, 6H), 3.63 (d, *J* = 12.5 Hz, 2H), 3.52 (d, *J* = 12.5 Hz, 2H), 2.49 (quin, *J* = 6.5 Hz, 1H), 2.01 (sext, *J* = 6.6 Hz, 1H), 1.11 (d, *J* = 6.5 Hz, 3H), 1.01 (d, *J* = 6.5 Hz, 3H), 0.95 (d, *J* = 6.6 Hz, 3H); ^{13}C NMR (100 MHz, $CDCl_3$) δ 159.2, 141.5, 140.2, 135.0, 133.5, 130.3, 128.2, 126.0, 125.8, 114.3, 64.2, 55.4, 52.1, 30.8, 21.0, 17.8, 13.2; IR (KBr) ν_{max} 3024, 2961, 2897, 2840, 1606, 1519, 1488, 1289, 1250, 1034, 882, 819 cm^{-1}; *m/z* (matrix: DTT/TG = 1/1) = 478 ([M+1]$^+$, 80%); Anal. Calcd for $C_{33}H_{35}NO_2$·1/10AcOEt: C, 82.47; H, 7.42; N, 2.88. Found: C, 82.40; H, 7.17; N, 2.96.

6-[(2*S*)-hexan-2-yl]-2,10-bis(4-methoxyphenyl)-6,7-dihydro-5*H*-dibenzo[*c*,*e*]azepine ((*S*)-5a)

Colorless oil: ^{1}H NMR (400 MHz, $CDCl_3$) δ 7.72 (d, *J* = 1.9 Hz, 2H), 7.60 (d, *J* = 8.7 Hz, 4H), 7.56 (dd, J_1 = 7.8 Hz, J_2 = 1.9 Hz ,2H), 7.44 (d, *J* = 7.8 Hz, 2H), 7.00 (d, *J* = 8.7 Hz, 4H), 3.86 (s, 6H), 3.62 (m, 4H), 2.82 (m, 1H), 1.69-1.37 (m, 6H), 1.15 (d, *J* = 6.5 Hz, 3H), 0.96-0.92 (m, 1H); ^{13}C NMR (100 MHz, $CDCl_3$) δ 159.2, 141.3, 140.3, 134.7, 133.4, 130.4, 128.2, 128.1, 125.8, 114.3, 58.9, 55.4, 51.8, 34.9, 28.9, 23.0, 17.7, 14.2; IR (KBr) ν_{max} 3033, 2953, 2929, 2854, 2834, 1608, 1517, 1488, 1287, 1246, 1032, 888, 818 cm^{-1}; *m/z* (matrix: DTT/TG = 1/1) = 492 ($[M+1]^+$, 40%); Anal. Calcd for $C_{34}H_{37}NO_2$: C, 83.06; H, 7.59; N, 2.85. Found: C, 83.21; H, 7.24; N, 2.75.

6-[(2*S*)-butan-2-yl]-2,10-bis(4-methoxyphenyl)-6,7-dihydro-5*H*-dibenzo[*c*,*e*]azepine ((*S*)-6a)

Colorless prisms: mp 152.6 °C (dec.); ^{1}H NMR (400 MHz, $CDCl_3$) δ 7.72 (d, *J* = 1.9 Hz, 2H), 7.60 (d, *J* = 8.8 Hz, 4H), 7.56 (dd, J_1 = 7.8 Hz, J_2 = 1.9 Hz ,2H), 7.43 (d, *J* = 7.8 Hz, 2H), 7.00 (d, *J* = 8.8 Hz, 4H), 3.86 (s, 6H), 3.63 (d, *J* = 12.5 Hz, 2H), 3.58 (d, *J* = 12.5 Hz, 2H), 2.73 (m, 1H), 1.77 (m, 1H), 1.52 (m, 1H), 1.20 (d, *J* = 6.5 Hz, 3H), 0.98 (t, *J* = 7.4 Hz, 9H); ^{13}C NMR (100 MHz, $CDCl_3$) δ 159.2, 141.5, 140.4, 140.4, 133.4,130.4, 128.2, 126.0, 125.8, 114.3, 60.1, 55.4, 51.8, 22.7, 17.3, 10.9; IR (KBr) ν_{max} 3025, 2962, 2936, 2838, 1608, 1518, 1489, 1290, 1248, 1025, 886, 820 cm^{-1}; *m/z* (matrix: DTT/TG = 1/1) = 465 ($[M+1]^+$, 95%); $C_{32}H_{33}NO_2$·1/10AcOEt: C, 82.37; H, 7.21; N, 2.97. Found: C, 82.27; H, 7.05; N, 2.98.

2,10-bis(4-methoxyphenyl)-6-[(1*S*)-1-phenylethyl]-6,7-dihydro-5*H*-dibenzo[*c*,*e*]azepine ((*S*)-7a)

White solid: mp 126.0 °C (dec.); ^{1}H NMR (400 MHz, $CDCl_3$) δ 7.71 (d, *J* = 1.8 Hz, 2H), 7.60 (d, *J* = 8.7 Hz, 4H), 7.55 (dd, J_1 = 7.8 Hz, J_2 = 1.8 Hz, 2H), 7.41 (d, *J* = 7.8 Hz, 2H), 6.99 (d, *J* = 8.7 Hz, 4H), 3.86 (s, 6H), 3.68 (d, *J* = 12.5 Hz, 2H), 3.57 (d, 12.5 Hz, 2H), 2.63 (q, *J* = 7.0 Hz, 1H), 1.14 (d, *J* = 7.0 Hz, 3H), 0.99 (s, 9H); ^{13}C NMR (100 MHz, $CDCl_3$) δ 159.3, 146.2, 141.7, 140.5, 133.8, 133.4, 130.3, 128.6, 128.2, 127.6, 127.0, 125.9, 125.9, 114.3, 62.6, 55.4, 52.9, 22.7; IR (KBr) ν_{max} 3024, 2965, 2930, 2832, 1607, 1517, 1488, 1282, 1247, 1032, 888, 818 cm^{-1}; *m/z* (matrix: DTT/TG = 1/1) = 512 ($[M+1]^+$, 30%); Anal. Calcd for $C_{36}H_{33}NO_2$: C, 84.51; H, 6.50; N, 2.74. Found: C, 84.61; H, 6.30; N, 2.62.

2,10-bis(4-methoxyphenyl)-6-[(1*S*)-1-(naphthalen-2-yl)ethyl]-6,7-dihydro-5*H*-dibenzo[*c*,*e*]azepin e ((*S*)-8a)

White Solid: mp 103.9 °C (dec.); ^{1}H NMR (400 MHz, $CDCl_3$) δ 7.91-7.86 (m, 4H), 7.74 (d, *J* = 1.8 Hz, 2H), 7.70 (d, *J* = 8.3 Hz, 1H), 7.61 (d, *J* = 8.8 Hz, 4H), 7.57 (dd, J_1 = 7.8 Hz, J_2 = 1.8 Hz, 2H), 7.52-7.45 (m, 2H), 7.37 (d, *J* = 7.8 Hz, 2H), 7.00 (d, *J* = 8.8 Hz, 4H), 3.86-3.82 (m, 7H), 3.65 (d, *J* = 12.5 Hz, 2H), 3.42 (d, 12.5 Hz, 2H), 1.57 (d, *J* = 6.5 Hz, 3H); ^{13}C NMR (100 MHz, $CDCl_3$) δ 159.3, 143.7, 141.7, 140.5, 133.8, 133.7, 133.6, 133.4, 132.9, 130.3, 128.5, 128.2, 127.8, 127.7, 126.0, 126.0, 125.9, 125.9, 114.3, 62.7, 55.4, 52.9, 22.7; IR (KBr) ν_{max} 3020, 2961, 2931, 2831, 1607, 1515, 1487, 1285, 1246, 1029, 888, 818, 746 cm^{-1}; *m/z* (matrix: DTT/TG = 1/1) = 563 ($[M+2]^+$, 15%); Anal. Calcd for $C_{40}H_{35}NO_2$: C, 85.53; H, 6.28; N, 2.49. Found: C, 85.32; H, 6.49; N, 2.41.

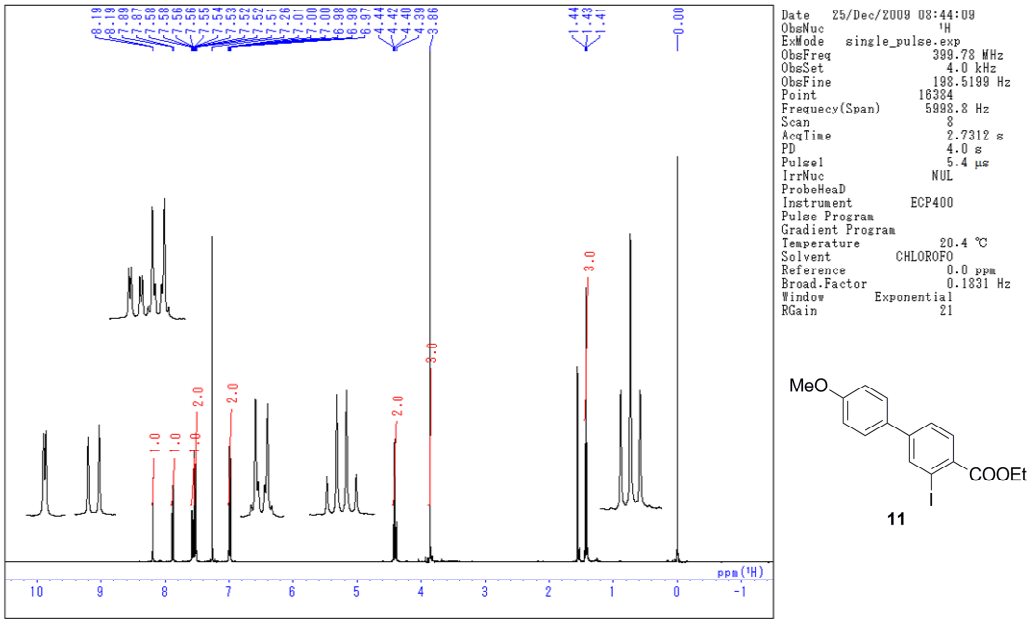

Figure S1. ^{1}H NMR Spectrum (400 MHz, $CDCl_3$) of **11**.

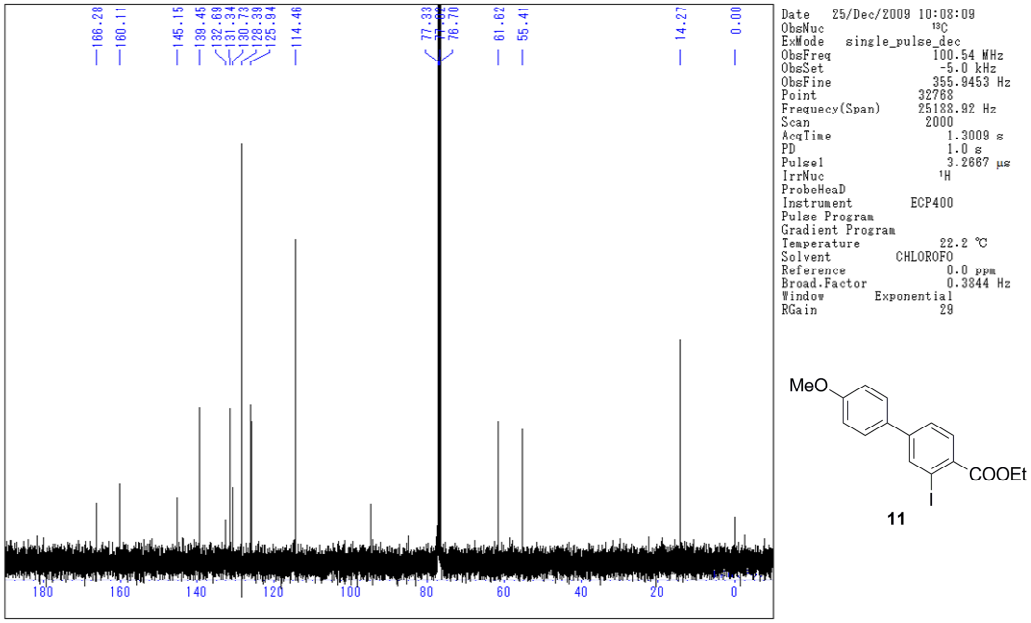

Figure S2. ^{13}C NMR Spectrum (100 MHz, $CDCl_3$) of **11**.

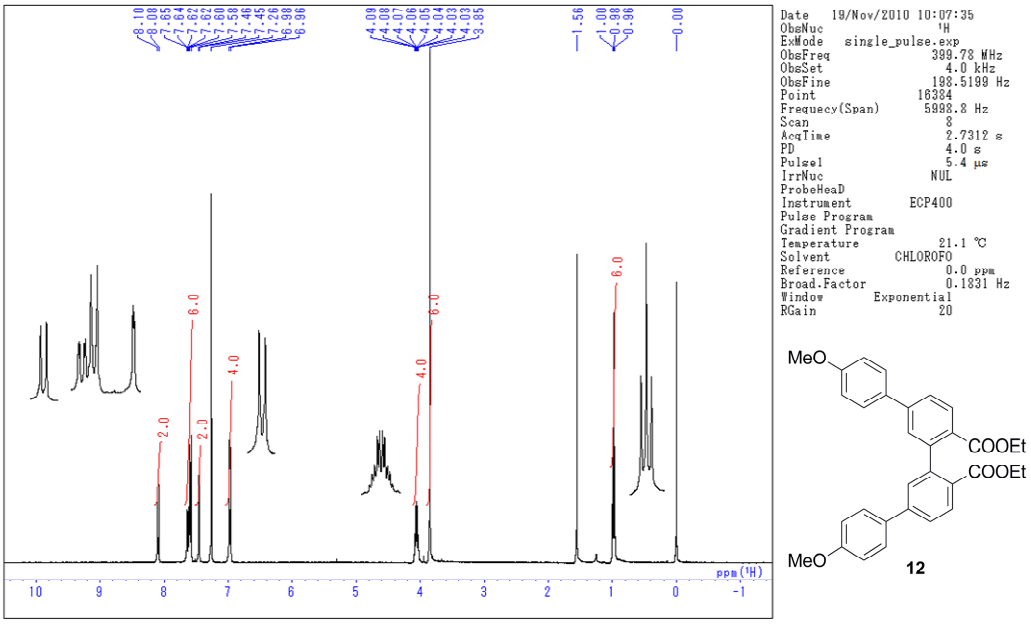

Figure S3. ^{1}H NMR Spectrum (400 MHz, $CDCl_3$) of **12**.

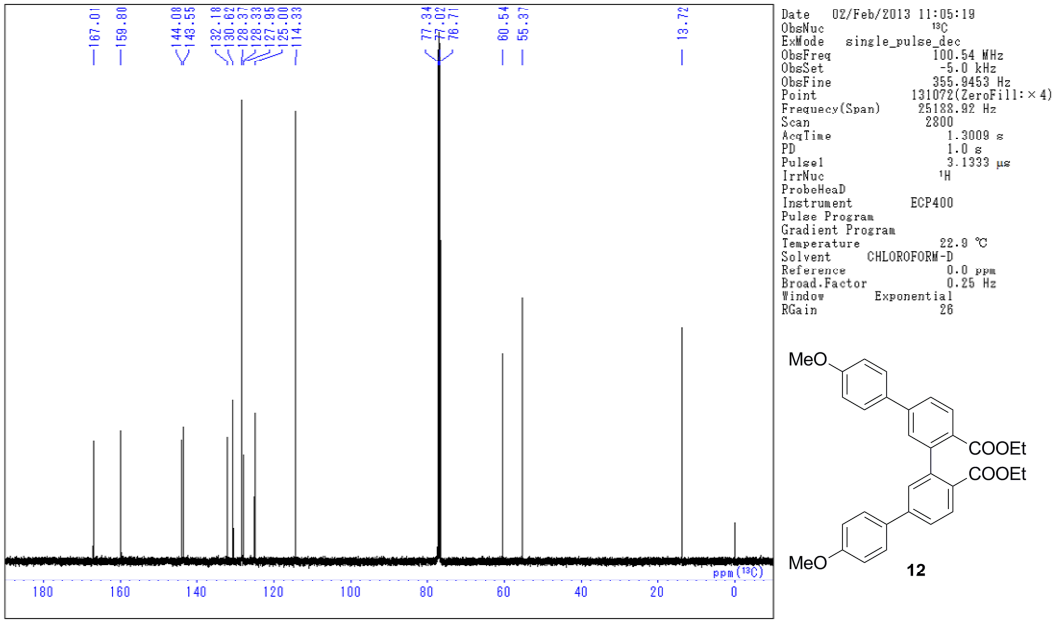

Figure S4. ^{13}C NMR Spectrum (100 MHz, $CDCl_3$) of **12**.

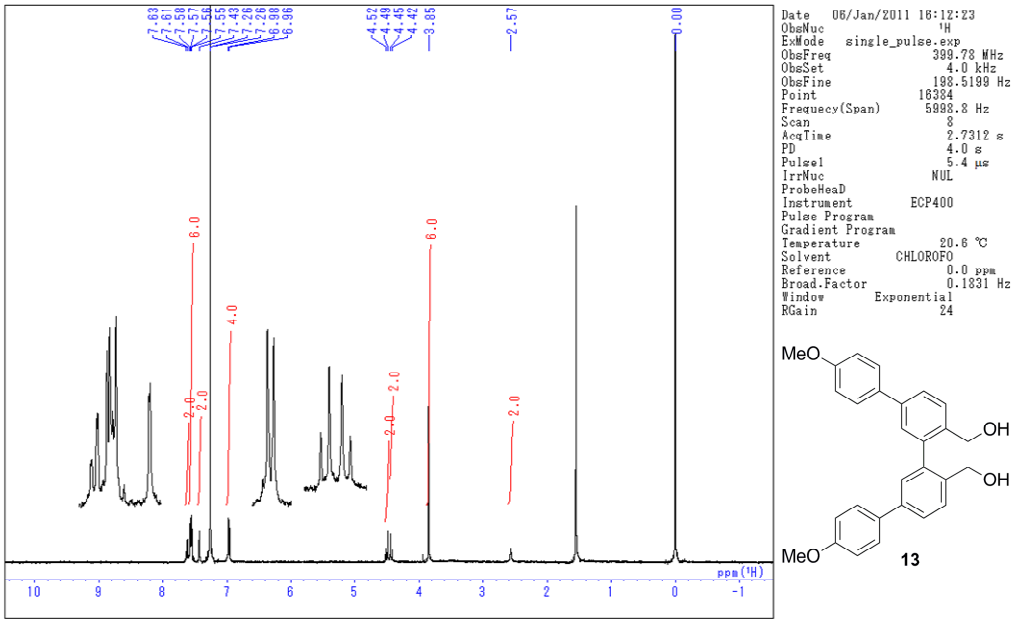

Figure S5. ^{1}H NMR Spectrum (400 MHz, $CDCl_3$) of **13**.

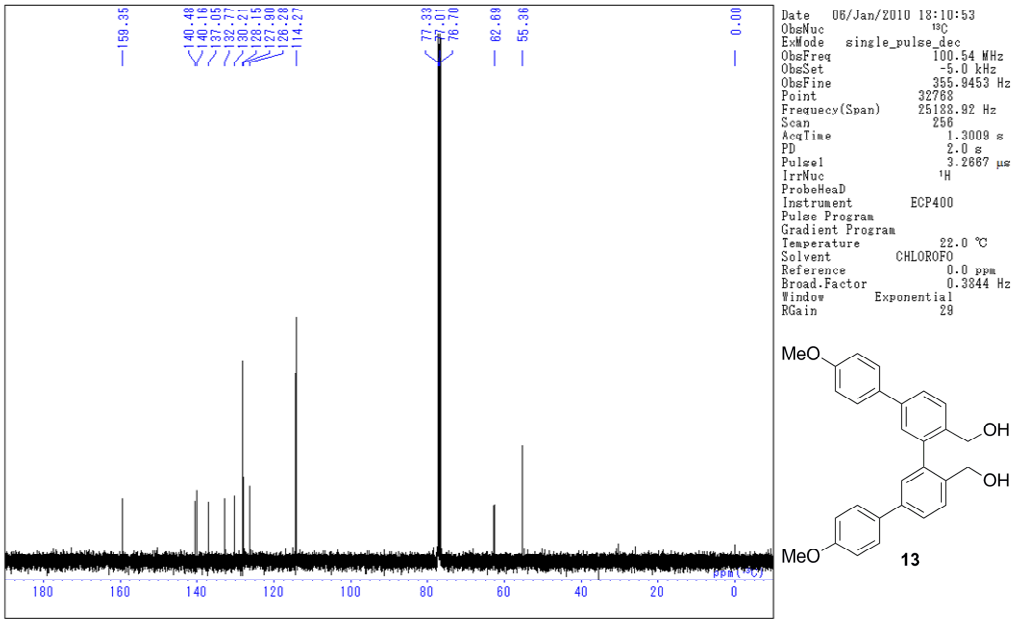

Figure S6. ^{13}C NMR Spectrum (100 MHz, $CDCl_3$) of **13**.

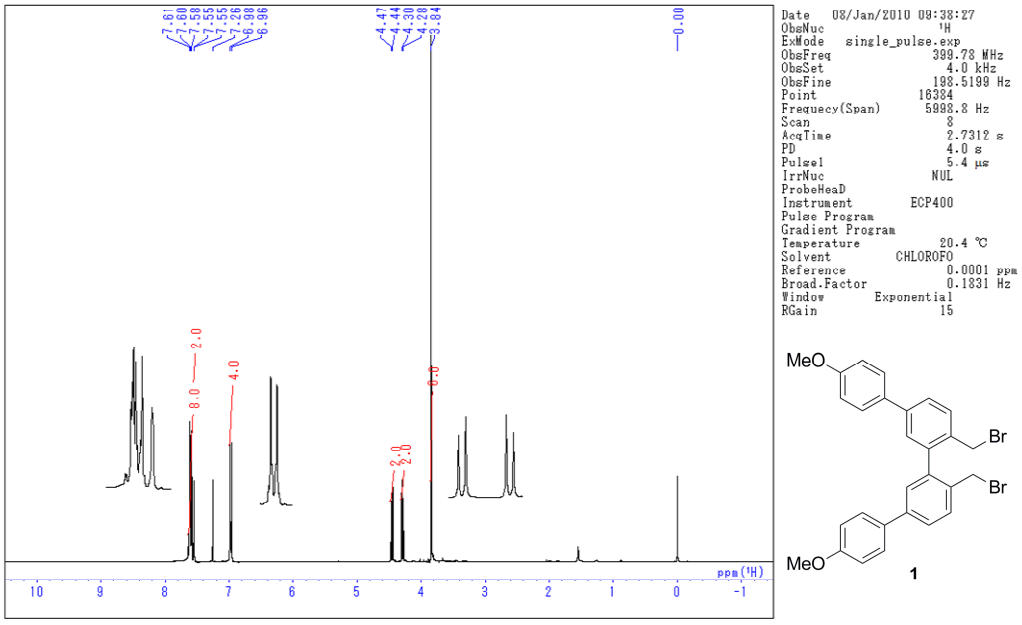

Figure S7 ^{1}H NMR Spectrum (400 MHz, $CDCl_3$) of **1**.

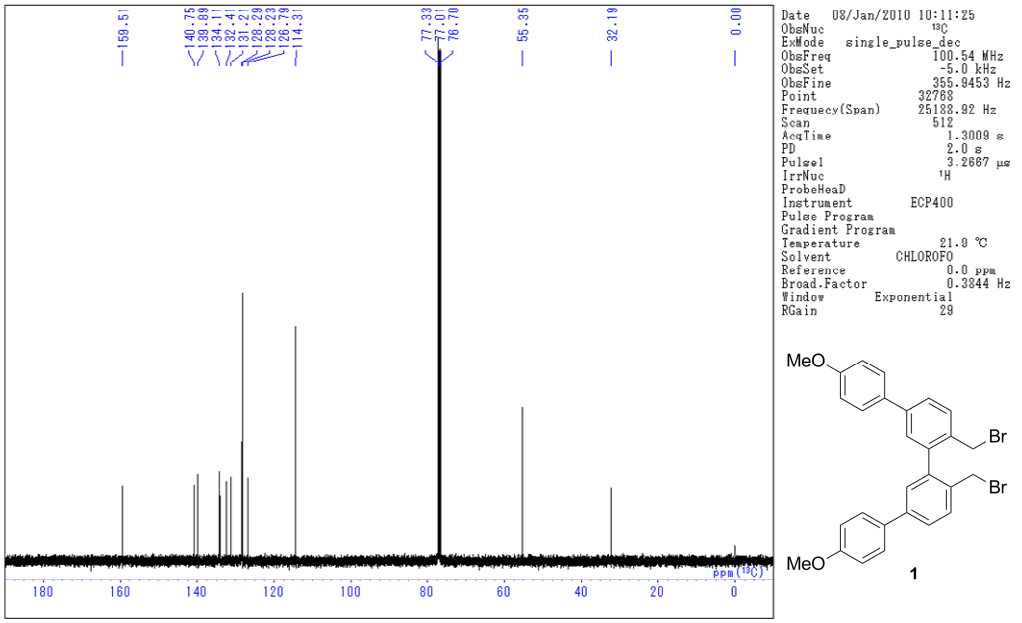

Figure S8. ^{13}C NMR Spectrum (100 MHz, $CDCl_3$) of **1**.

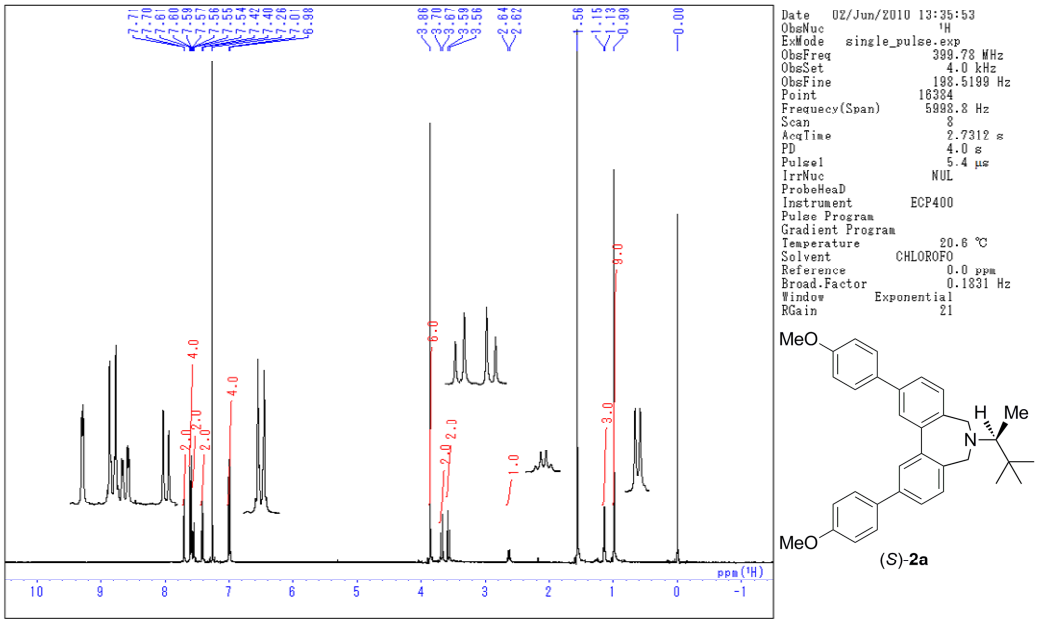

Figure S9. ^{1}H NMR Spectrum (400 MHz, $CDCl_3$) of (*S*)-**2a**.

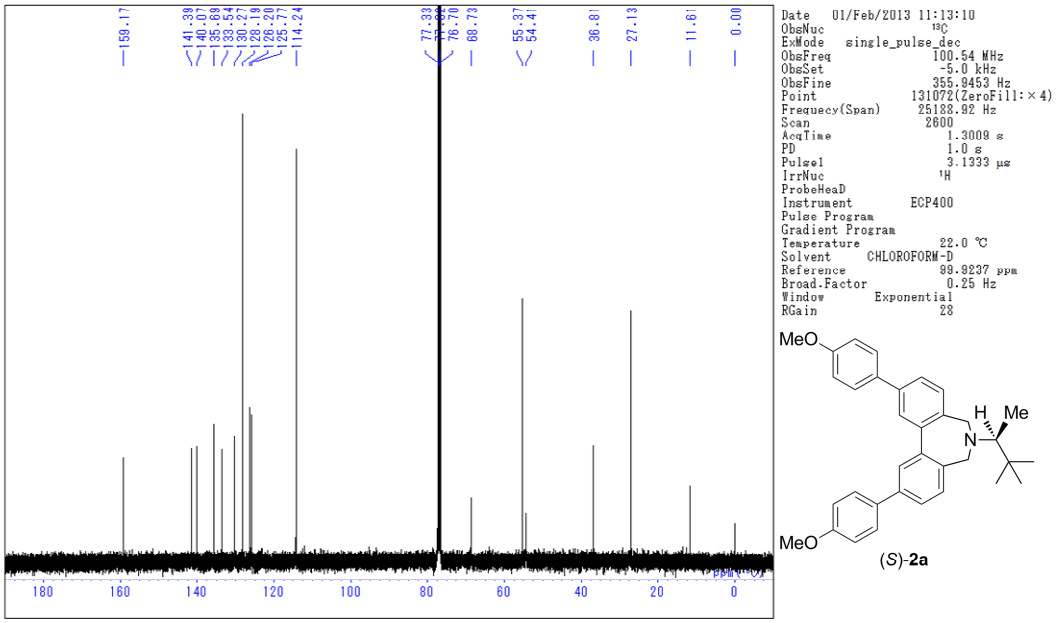

Figure S10. ^{13}C NMR Spectrum (100 MHz, $CDCl_3$) of (*S*)-**2a**.

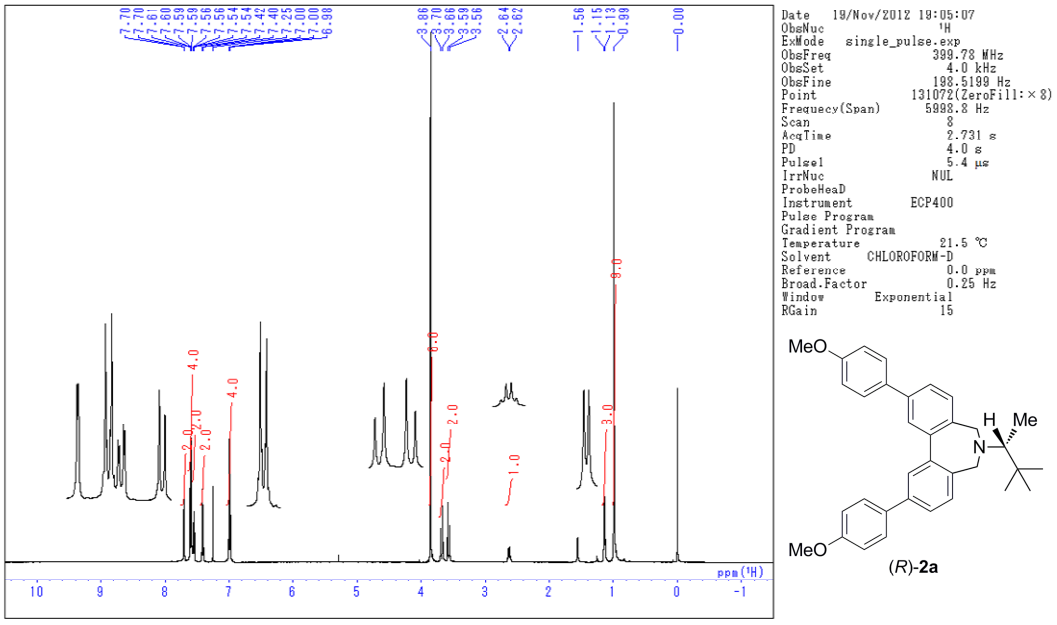

Figure S11. ^{1}H NMR Spectrum (400 MHz, $CDCl_3$) of (*R*)-**2a**.

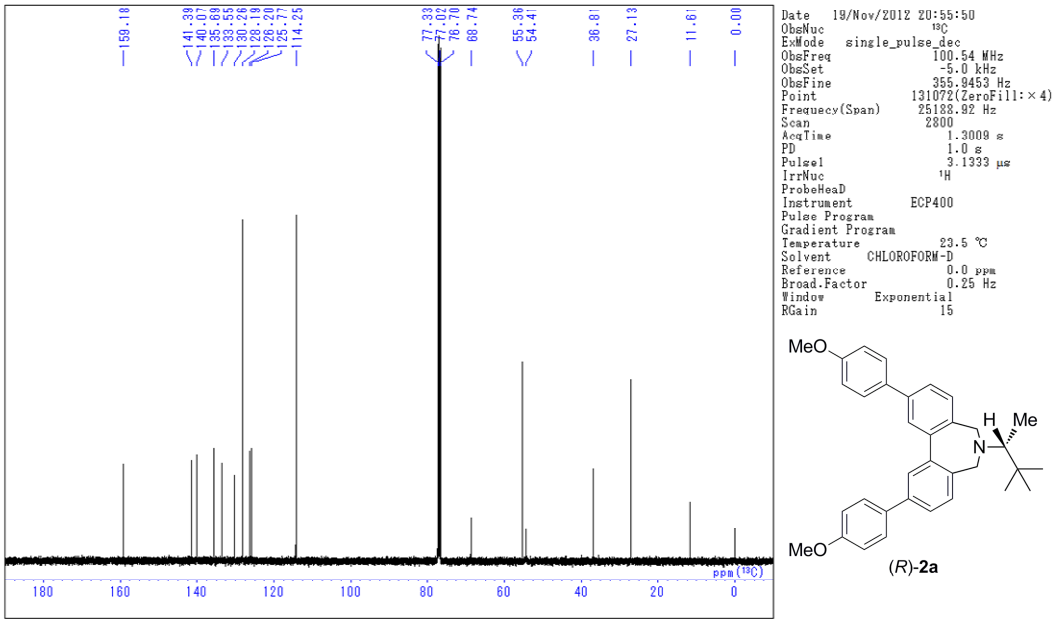

Figure S12. ^{13}C NMR Spectrum (100 MHz, $CDCl_3$) of (*R*)-**2a**.

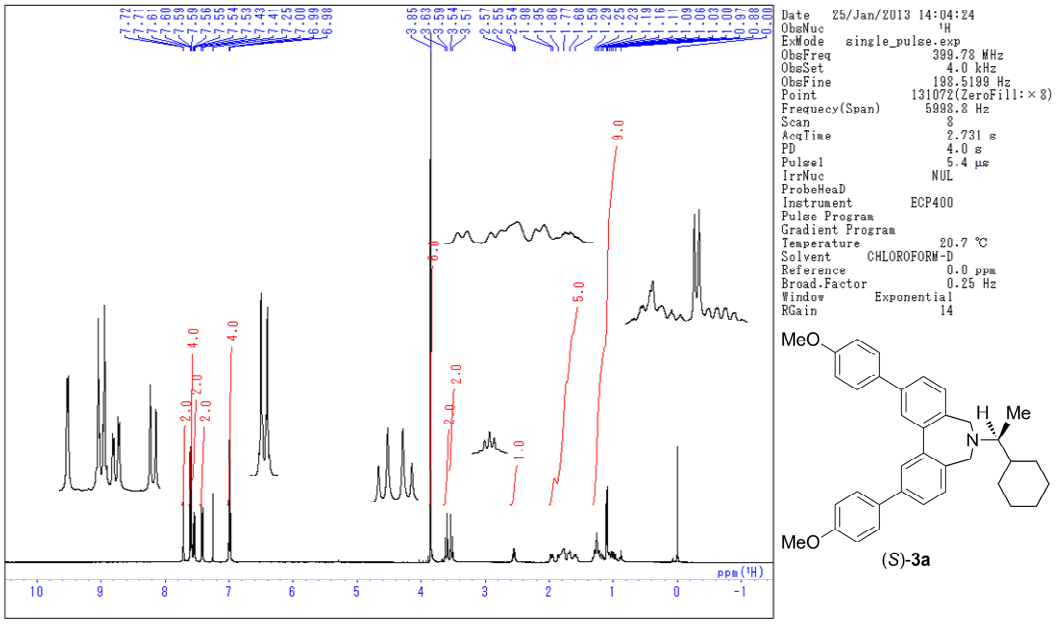

Figure S13. ^{1}H NMR Spectrum (400 MHz, $CDCl_3$) of (*S*)-**3a**.

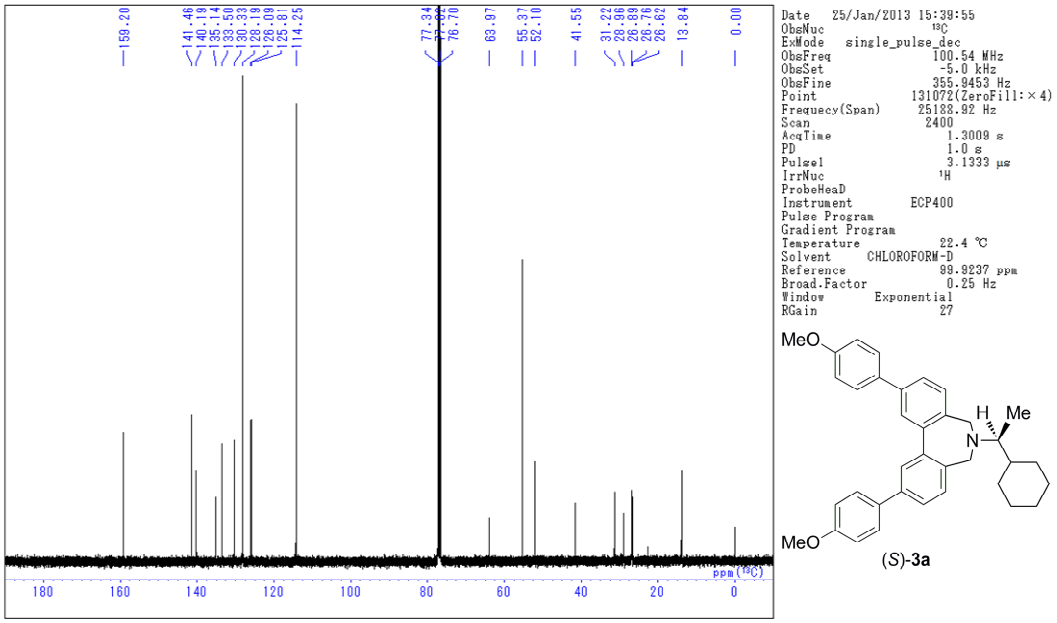

Figure S14. ^{13}C NMR Spectrum (100 MHz, $CDCl_3$) of (*S*)-**3a**.

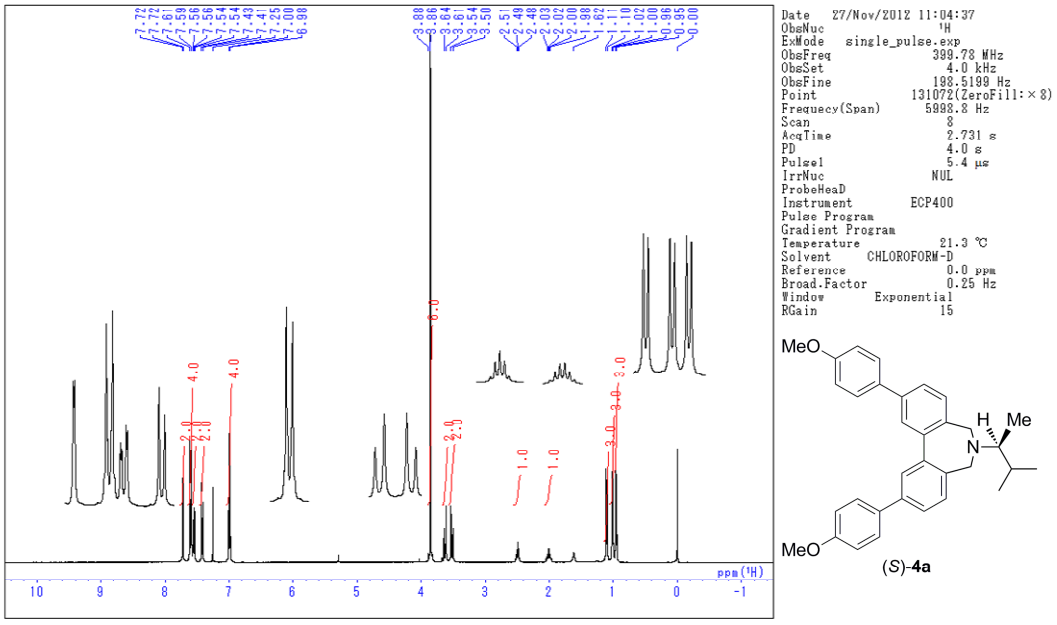

Figure S15. ^{1}H NMR Spectrum (400 MHz, $CDCl_3$) of (*S*)-**4a**.

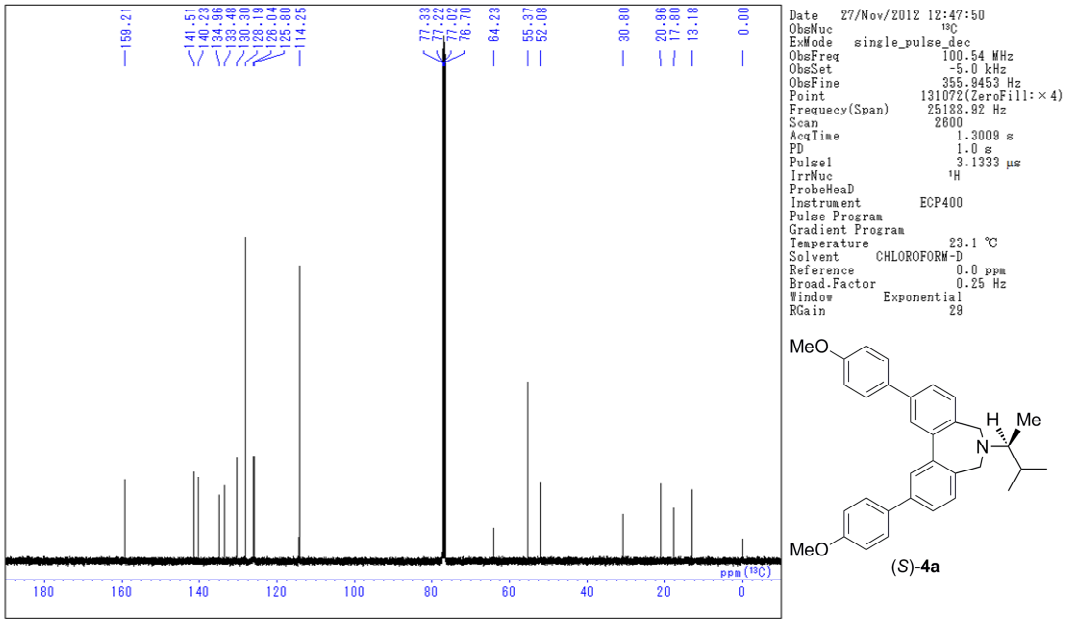

Figure S16. ^{13}C NMR Spectrum (100 MHz, $CDCl_3$) of (*S*)-**4a**.

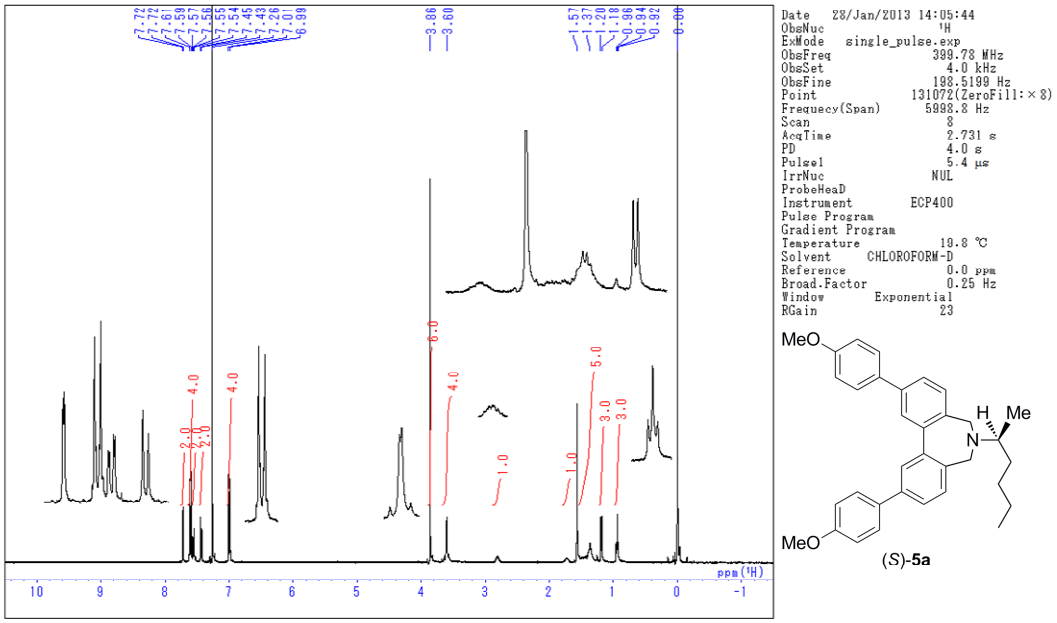

Figure S17. ^{1}H NMR Spectrum (400 MHz, $CDCl_3$) of (*S*)-**5a**.

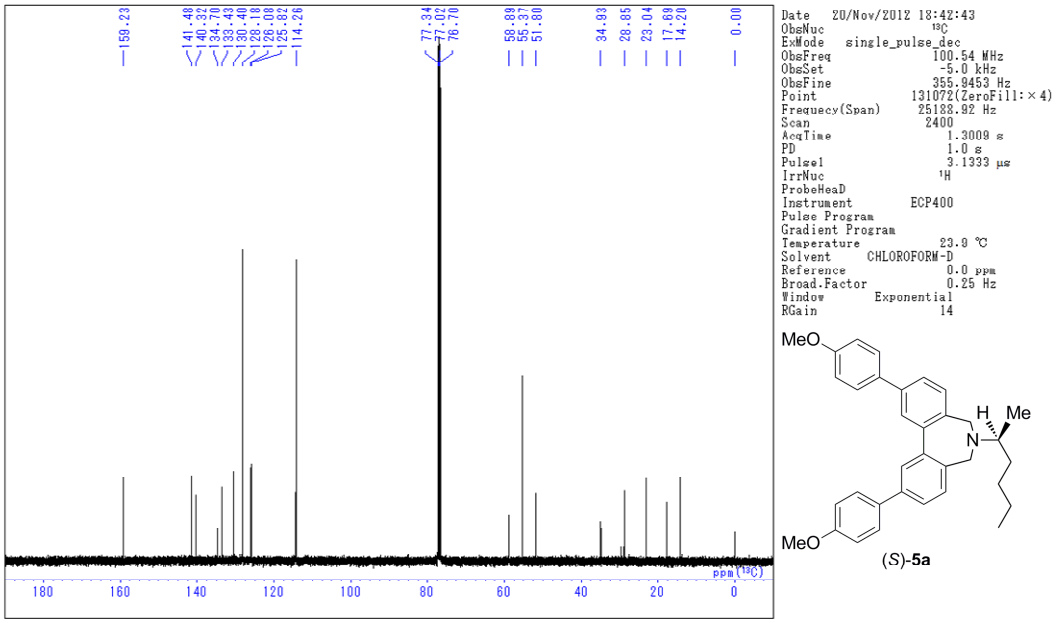

Figure S18. ^{13}C NMR Spectrum (100 MHz, $CDCl_3$) of (*S*)-**5a**.

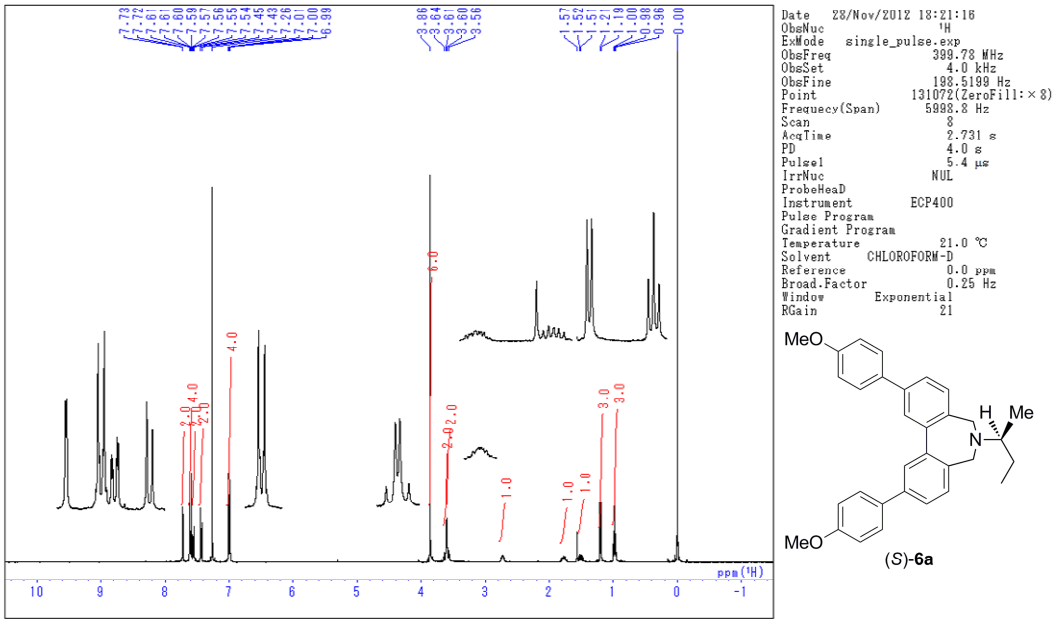

Figure S19. ^{1}H NMR Spectrum (400 MHz, $CDCl_3$) of (*S*)-**6a**.

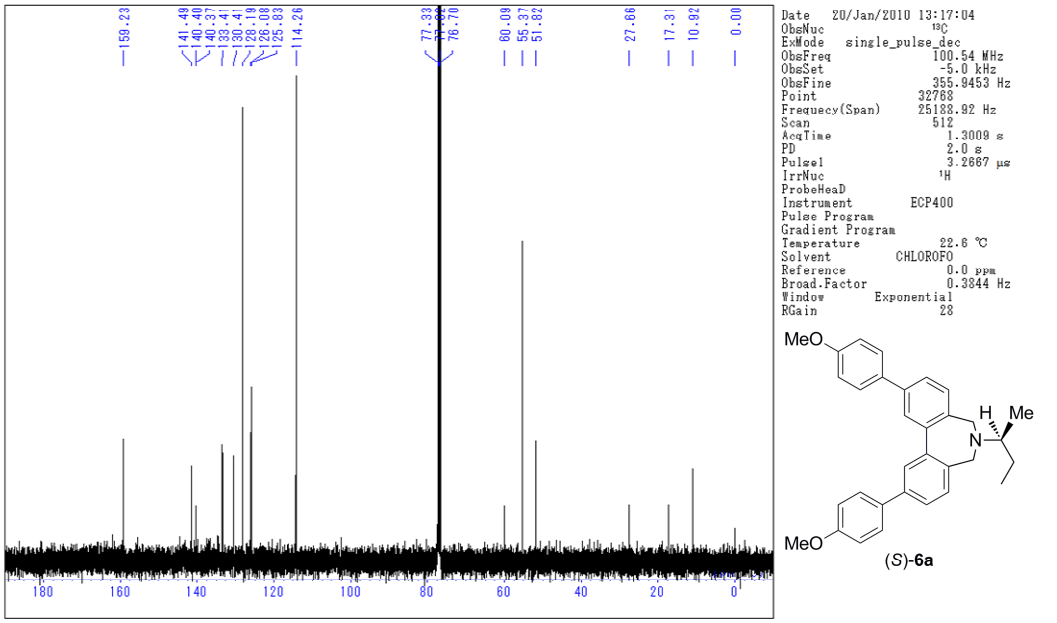

Figure S20. ^{13}C NMR Spectrum (100 MHz, $CDCl_3$) of (*S*)-**6a**.

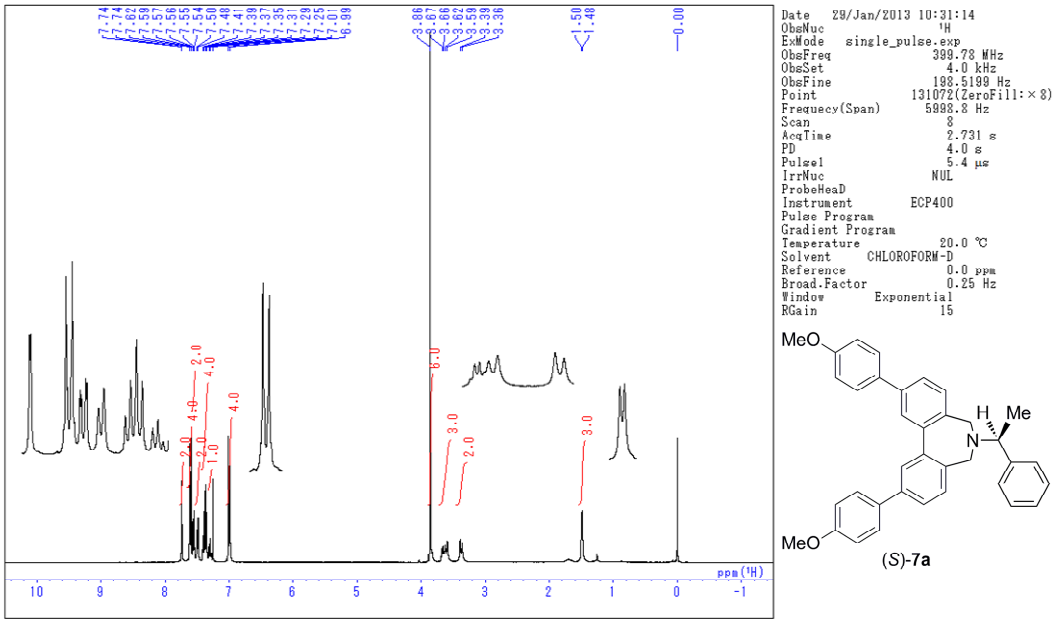

Figure S21. ^{1}H NMR Spectrum (400 MHz, $CDCl_3$) of (*S*)-**7a**.

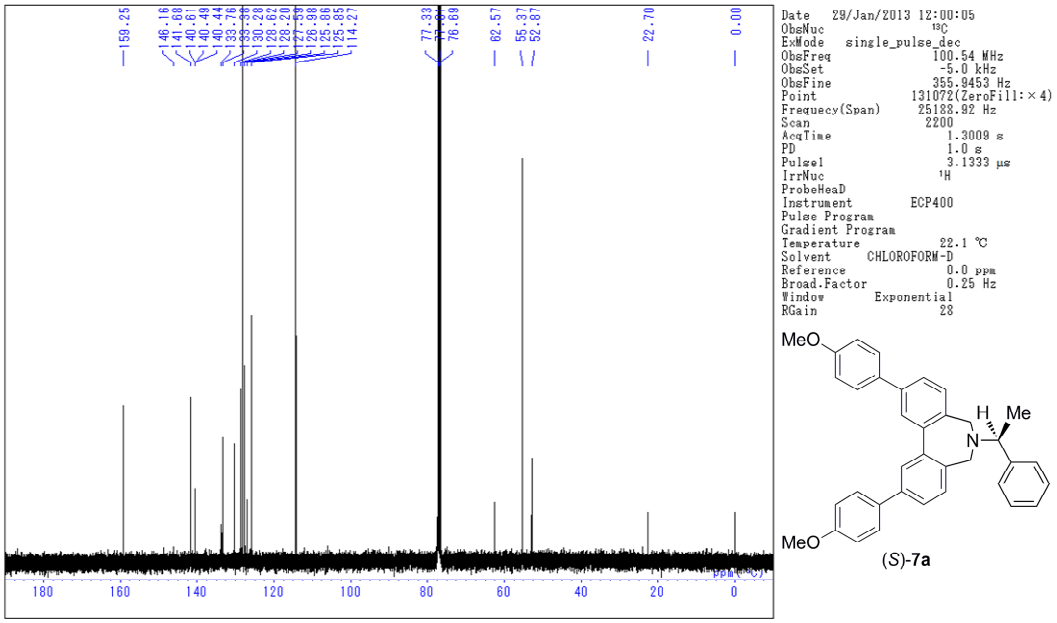

Figure S22. ^{13}C NMR Spectrum (100 MHz, $CDCl_3$) of (*S*)-**7a**.

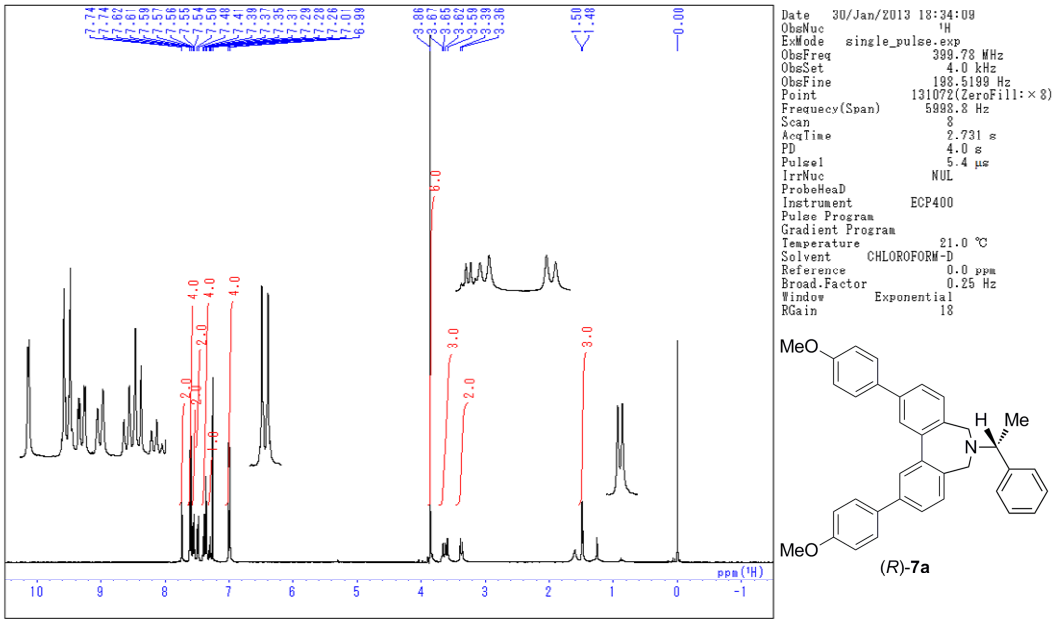

Figure S23. ^{1}H NMR Spectrum (400 MHz, $CDCl_3$) of (*R*)-**7a**.

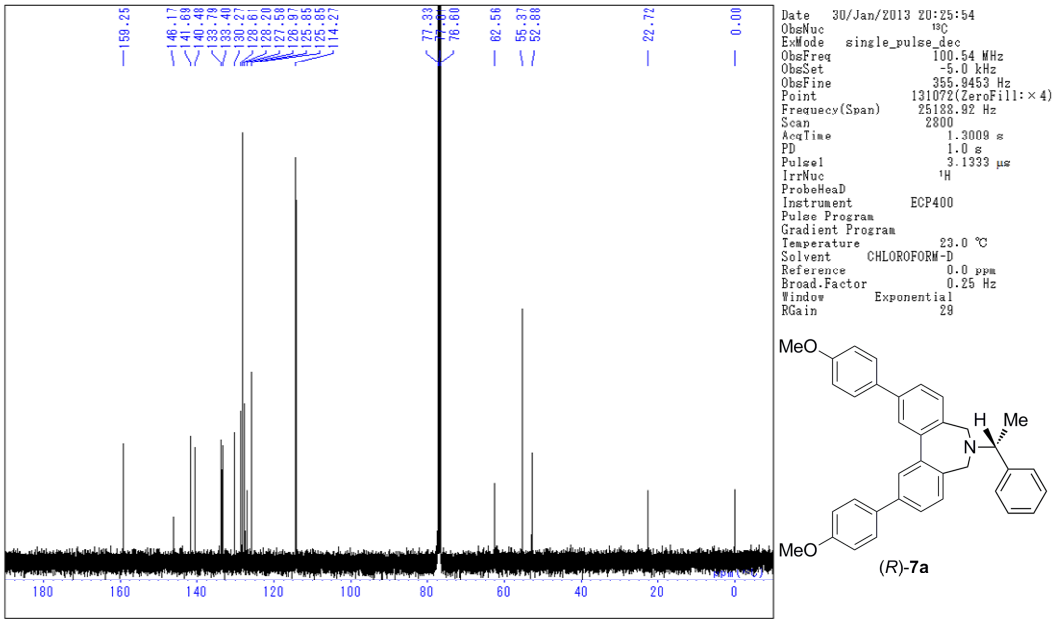

Figure S24. ^{13}C NMR Spectrum (100 MHz, $CDCl_3$) of (*R*)-**7a**.

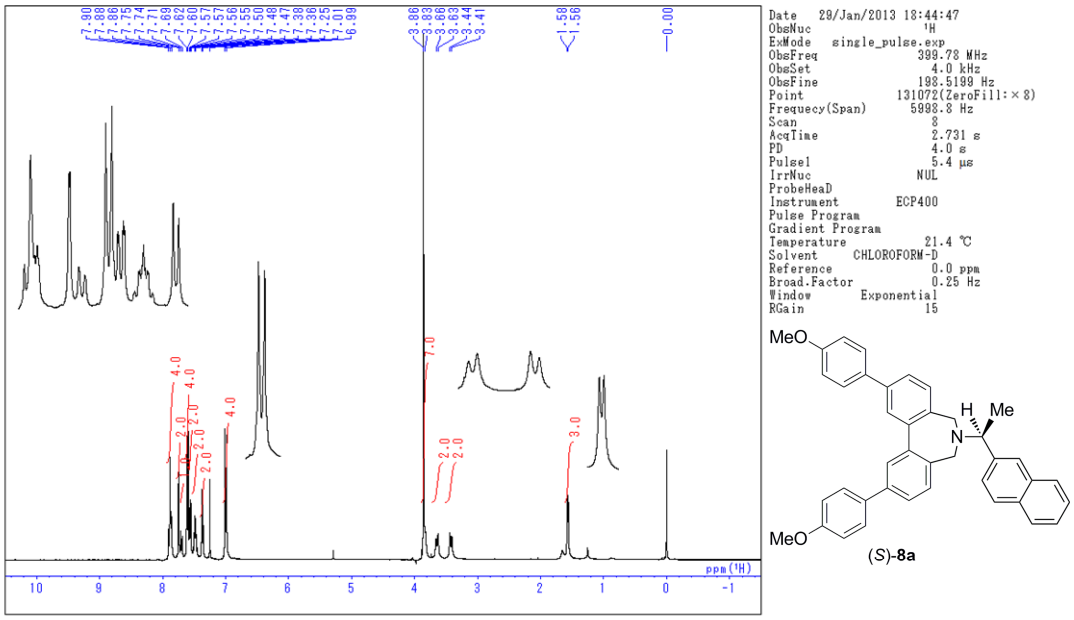

Figure S25. ^{1}H NMR Spectrum (400 MHz, $CDCl_3$) of (*S*)-**8a**.

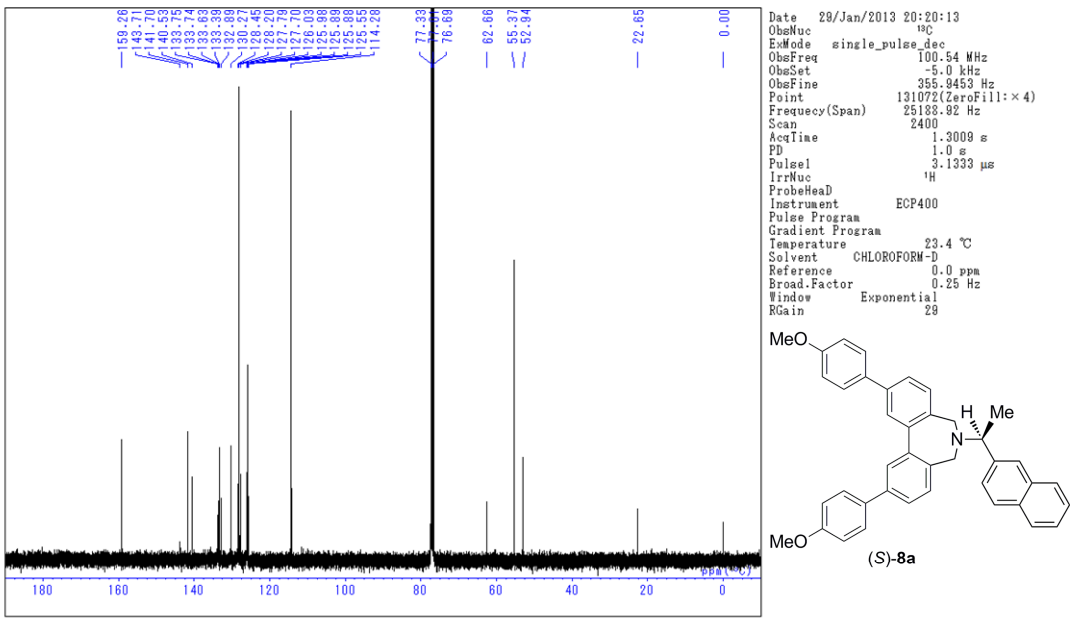

Figure S26. ^{13}C NMR Spectrum (100 MHz, $CDCl_3$) of (*S*)-**7a**.

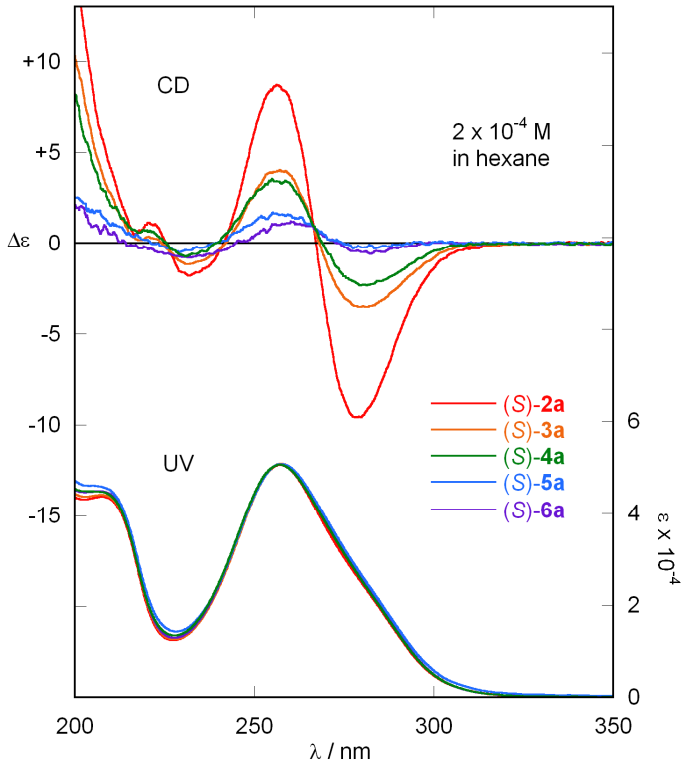

Figure S27. CD and UV Spectra of aliphatic amines (*S*)-**2a–6a** (2 x 10^{-4} M in hexane, 293 K).

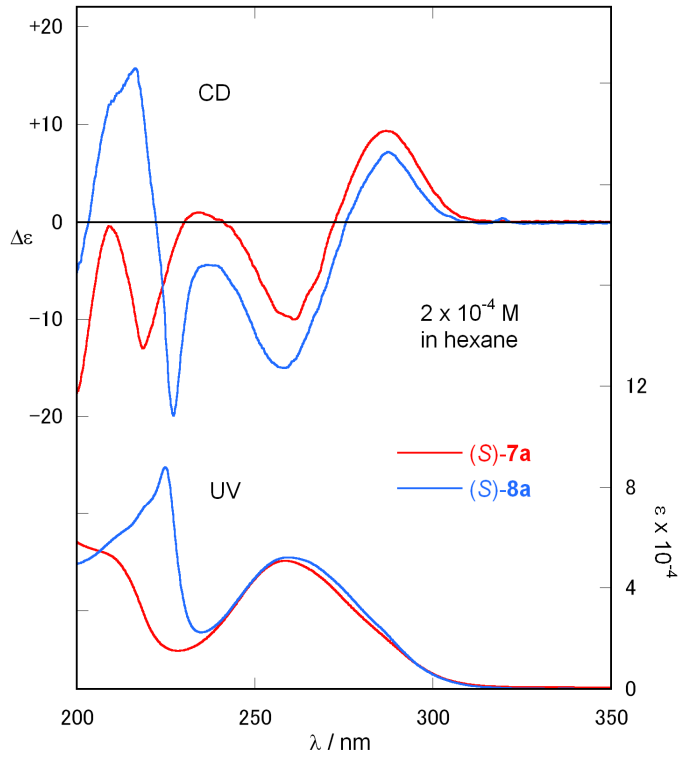

Figure S28. CD and UV Spectra of aromatic amines (*S*)-**7a** and (*S*)-**8a** (2 x 10^{-4} M in hexane, 293 K).

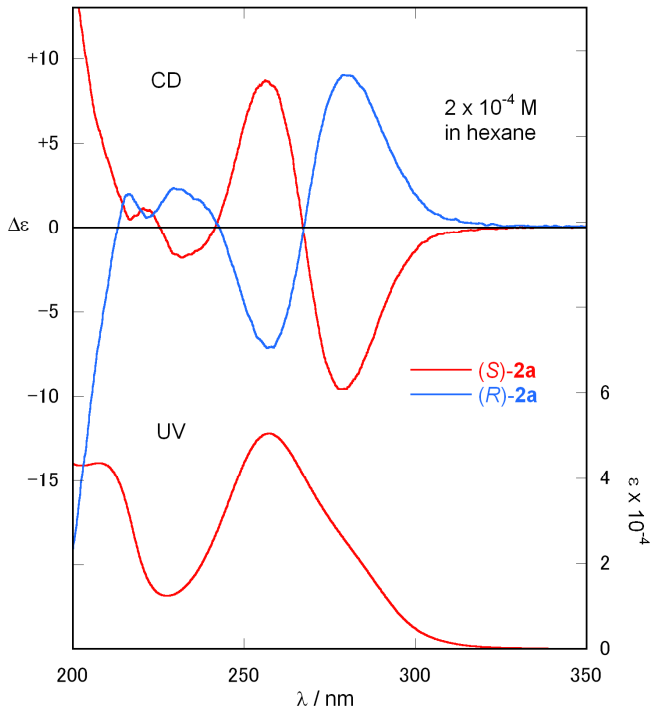

Figure S29. CD and UV Spectra of (*S*)-**2a** and (*R*)-**2a** (2 x 10^{-4} M in hexane, 293 K).

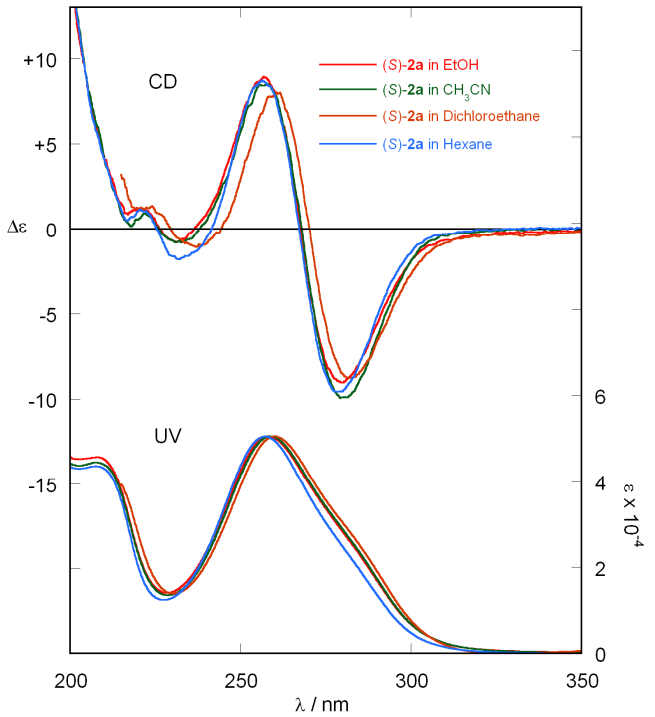

Figure S30. CD and UV Spectra of (*S*)-**2a** with varying solvents (2 x 10^{-4} M, 293 K).

Table S1. CD spectral data of (*S*)-**2a**–(*S*)-**8a**[a].

Entry	Compound	$\Delta\varepsilon_1$[b] (λ [nm])	$\Delta\varepsilon_2$[b] (λ [nm])	CD amplitude (A_{CD} value)[c]
1	(*S*)-**2a**	–9.2 (278.8)	+8.5 (256.2)	–17.7
2	(*S*)-**3a**	–3.5 (279.4)	+4.0 (257.2)	–7.5
3	(*S*)-**4a**	–2.4 (281.4)	+3.5 (255.0)	–5.9
4	(*S*)-**5a**	–0.3 (283.6)	+1.6 (255.2)	–1.9
5	(*S*)-**6a**	–0.6 (282.6)	+1.2 (260.2)	–1.8
6	(*S*)-**7a**	+9.8 (286.8)	–10.6 (261.2)	+20.4
7	(*S*)-**8a**	+7.2 (287.4)	–15.0 (258.4)	+22.2

[a] All CD data were measured in hexane, 2 x 10^{-4} M concentration using 1 mm CD cell at 293 K. [b] $\Delta\varepsilon_1$ and $\Delta\varepsilon_2$ are intensities of first and second Cotton effects. [c] A_{CD} value: $A_{CD} = \Delta\varepsilon_1 - \Delta\varepsilon_2$, where $\Delta\varepsilon_1$ and $\Delta\varepsilon_2$ are intensities of first and second Cotton effects, respectively.

Theoretical calculations

To obtain the population between *M* and *P* conformers, preliminary conformational searches were run on the structure of (*S*)-**2b**–(*S*)-**4b** and (*S*)-**6b**–(*S*)-**8b** using MMFF. All local minimum conformers were then optimized with DFT using B3LYP/6-31G* model. The lower energy conformers with relative energies ranging from 0.0 to 3.0 kcal/mol were selected. By the Bolzmann distribution based on the energy difference of the conformers at 293 K, the population of the *M* and *P* conformers were determined. Calculations using HF/6-31G* also gave similar results.

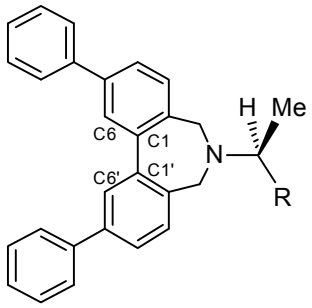

(*S*)-**2b** : R = *t*-Bu
(*S*)-**3b** : R = cyclohexyl
(*S*)-**4b** : R = *i*-Pr
(*S*)-**5b** : R = *n*-Bu
(*S*)-**6b** : R = Et
(*S*)-**7b** : R = Ph
(*S*)-**8b** : R = 2-Naph

Figure S31. Methoxy-omitted model of **1**-amine conjugates for theoretical calculations.

Theoretical calculations at B3LYP/6-31G* level

Table S2. Calculated conformers of (*S*)-**2b** at B3LYP/6-31G* level.

Entry	Conformer	Dihedral angle[a]	Δ*E*, kcal/mol	*K*[b]	Population, %
1	#M3	-42.75	0.00	1.00	42.9
2	#M1	-42.20	0.17	0.75	32.3
3	#P1	43.53	0.32	0.58	24.8

[a] Dihedral angle of C6-C1-C1'-C6'. [b] Equilibrium constant at 293 K.

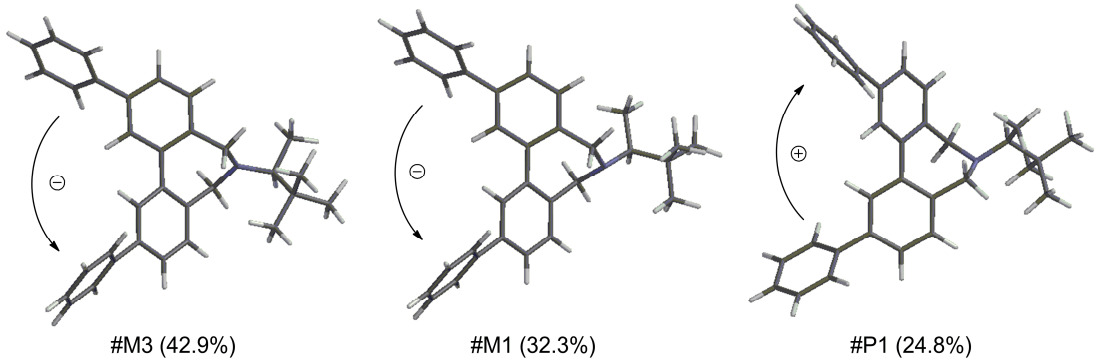

Figure S32. Three major conformers of (*S*)-**2b** at B3LYP/6-31G* level.

Table S3. Calculated conformers of (*S*)-**3b** at B3LYP/6-31G* level.

Entry	Conformer	Dihedral angle[a]	Δ*E*, kcal/mol	*K*[b]	Population, %
1	#M1	-42.32	0.00	1.00	46.8
2	#P1	42.86	0.14	0.79	36.9
3	#P3	42.24	1.63	0.06	2.9
4	#M7	-42.17	1.66	0.06	2.7
5	#M5	-42.65	1.69	0.05	2.6
6	#M20	-42.63	1.93	0.04	1.7
7	#P5	43.25	1.97	0.03	1.6
8	#M3	-42.78	2.11	0.03	1.2
9	#P20	42.95	2.17	0.02	1.1
10	#P7	43.57	2.21	0.02	1.0
11	#P9	44.15	2.61	0.01	0.5
12	#M15	-44.15	2.85	0.01	0.4
13	#M13	-43.13	2.86	0.01	0.3
14	#M9	-42.33	2.89	0.01	0.3

[a] Dihedral angle of C6-C1-C1'-C6'. [b] Equilibrium constant at 293 K.

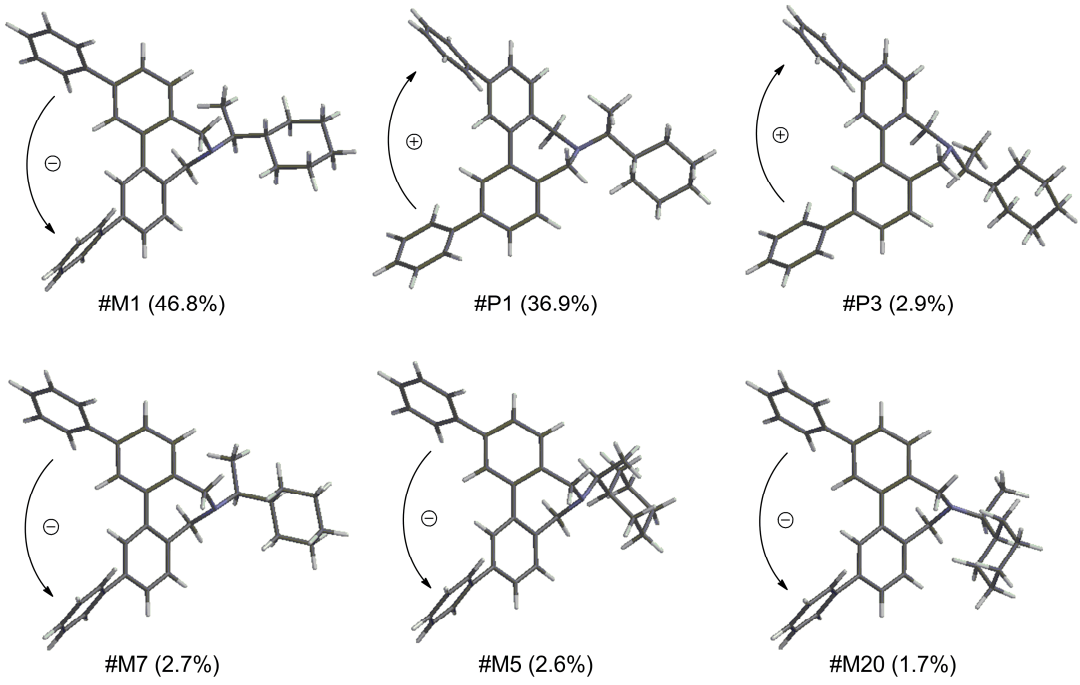

Figure S33. Six major conformers of (*S*)-**3b** at B3LYP/6-31G* level.

Table S4. Calculated conformers of (*S*)-**4b** at B3LYP/6-31G* level.

Entry	Conformer	Dihedral angle[a]	Δ*E*, kcal/mol	*K*[b]	Population, %
1	#M1	-42.99	0.00	1.00	50.3
2	#P1	41.67	0.20	0.71	35.5
3	#P3	42.18	1.34	0.10	5.1
4	#M3	-42.63	1.44	0.08	4.2
5	#M5	-43.14	1.70	0.05	2.7
6	#P5	42.55	2.10	0.03	1.4
7	#M7	-42.17	2.70	0.01	0.5
8	#P7	44.46	2.78	0.01	0.4

[a] Dihedral angle of C6-C1-C1'-C6'. [b] Equilibrium constant at 293 K.

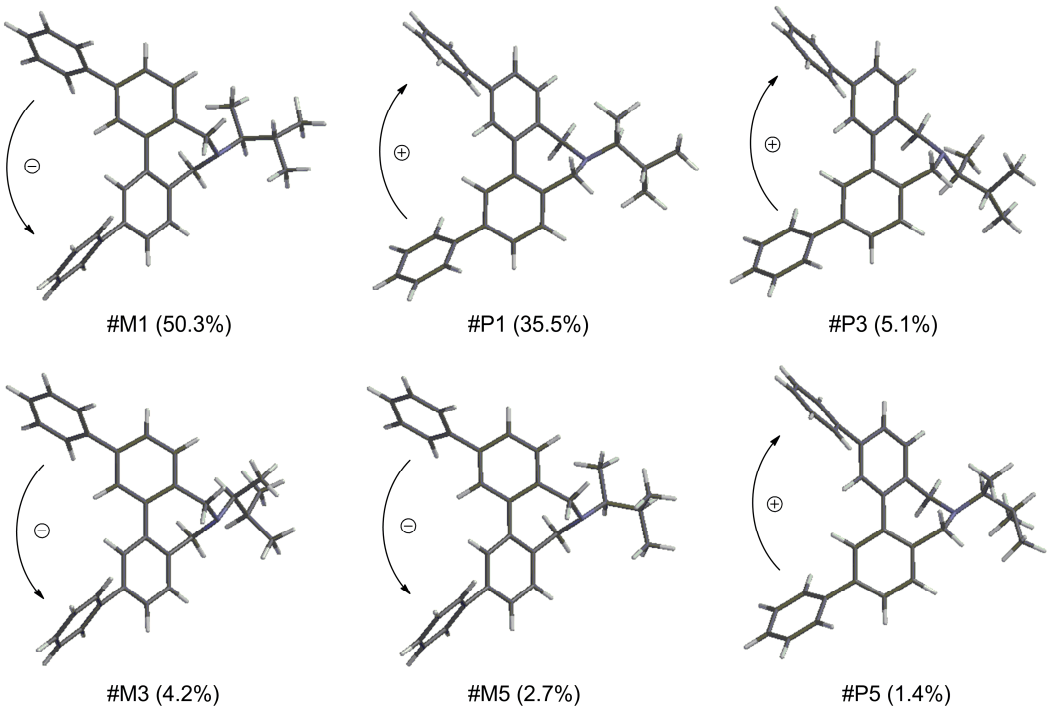

Figure S34. Six major conformers of (*S*)-**4b** at B3LYP/6-31G* level.

Table S5. Calculated conformers of (*S*)-**6b** at B3LYP/6-31G* level.

Entry	Conformer	Dihedral angle[a]	Δ*E*, kcal/mol	*K*[b]	Population, %
1	#M1	-42.56	0.00	1.00	35.5
2	#P1	43.48	0.18	0.74	26.2
3	#P5	41.94	0.79	0.26	9.1
4	#M5	-43.25	0.91	0.21	7.4
5	#P7	42.96	1.03	0.17	6.1
6	#M7	-41.95	1.12	0.15	5.2
7	#M3	-43.35	1.32	0.10	3.7
8	#P3	43.56	1.36	0.10	3.4
9	#P9	42.47	1.88	0.04	1.4
10	#P11	42.76	2.12	0.03	0.9
11	#M9	-41.92	2.28	0.02	0.7
12	#M11	-43.63	2.58	0.01	0.4

[a] Dihedral angle of C6-C1-C1'-C6'. [b] Equilibrium constant at 293 K.

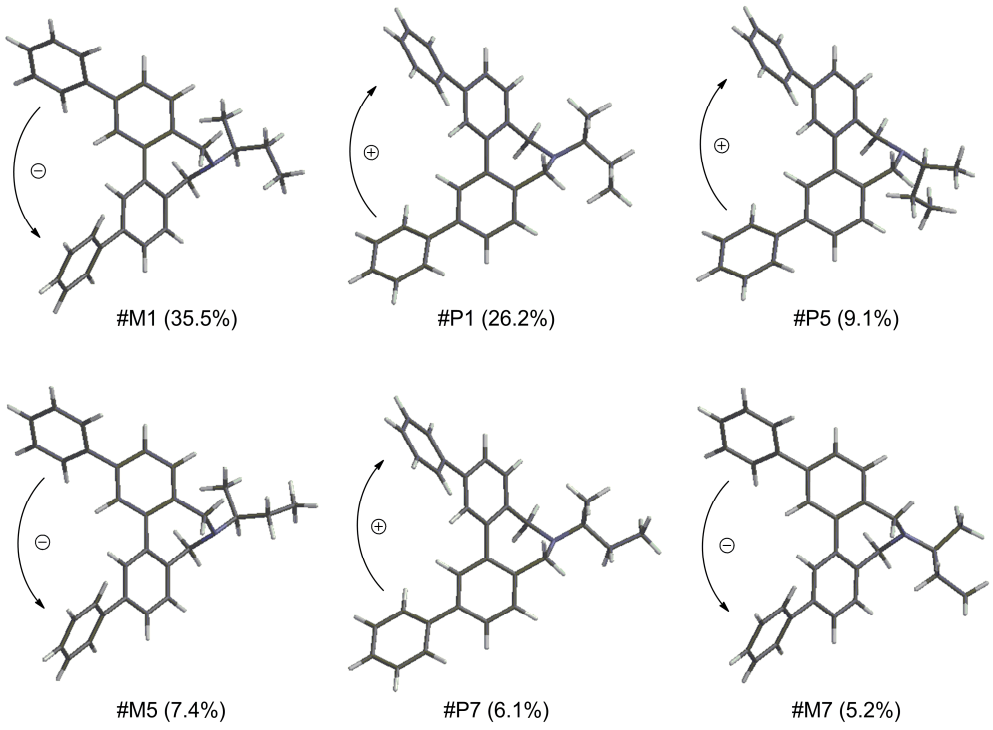

Figure S35. Six major conformers of (*S*)-**6b** at B3LYP/6-31G* level.

Table S6. Calculated conformers of (*S*)-**7b** at B3LYP/6-31G* level.

Entry	Conformer	Dihedral angle[a]	Δ*E*, kcal/mol	*K*[b]	Population, %
1	#P1	42.27	0.00	1.00	66.7
2	#M1	-42.94	0.49	0.43	28.5
3	#M5	-42.64	1.91	0.04	2.5
4	#P3	42.66	1.96	0.03	2.3

[a] Dihedral angle of C6-C1-C1'-C6'. [b] Equilibrium constant at 293 K.

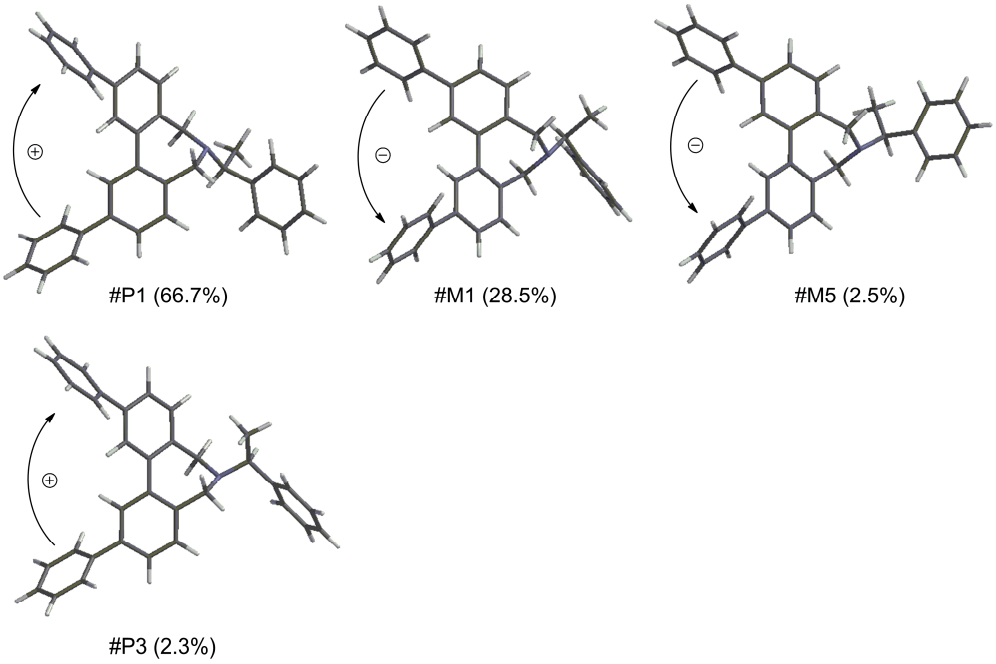

Figure S36. Four major conformers of (*S*)-**6b** at B3LYP/6-31G* level.

Table S7. Calculated conformers of (*S*)-**8b** at B3LYP/6-31G* level.

Entry	Conformer	Dihedral angle[a]	Δ*E*, kcal/mol	*K*[b]	Population, %
1	#P1	43.06	0.00	1.00	39.5
2	#P3	41.89	0.06	0.90	35.7
3	#M3	-41.45	0.78	0.26	10.3
4	#M1	-43.24	0.86	0.23	9.0
5	#M7	-42.87	1.43	0.09	3.4
6	#P5	43.86	1.70	0.05	2.1

[a] Dihedral angle of C6-C1-C1'-C6'. [b] Equilibrium constant at 293 K.

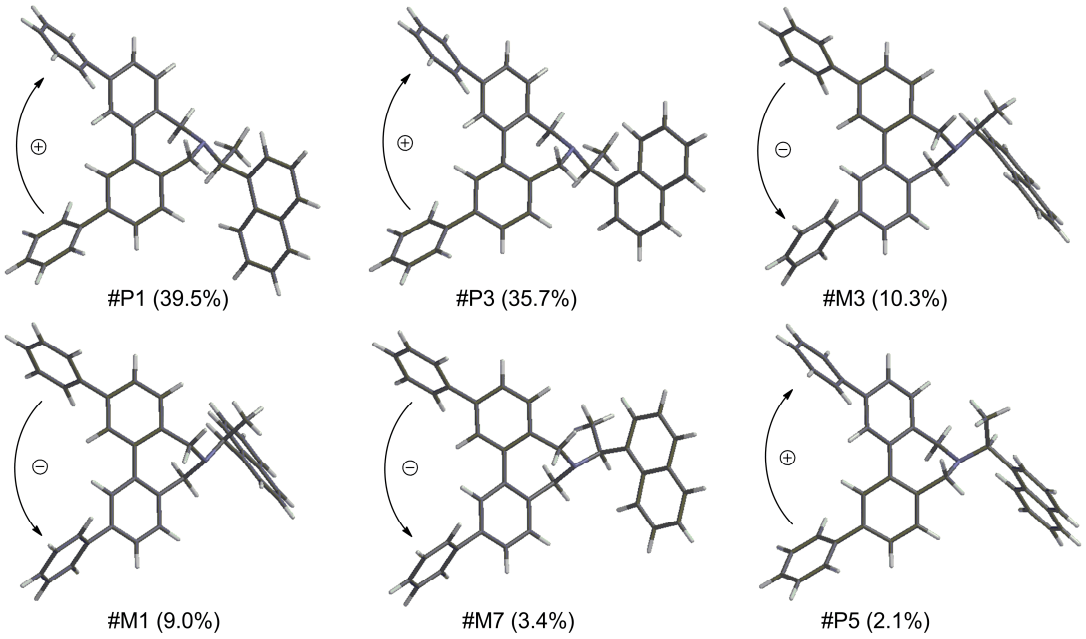

Figure S37. Six major conformers of (*S*)-**6b** at B3LYP/6-31G* level.

Table S8. Comparison of the excess of *M* conformer and observed CD amplitude at B3LYP/6-31G* level.

Entry	Compound	Calcurated ratio (*M*/*P*)	Excess of *M* confomer, %[a]	Observed CD amplitude (A_{CD} value)[b]
1	(*S*)-**2b**	75.2:24.8	50.4	-17.7 ((*S*)-**2a**)
2	(*S*)-**3b**	56.0:44.0	12.0	-7.5 ((*S*)-**3a**)
3	(*S*)-**4b**	57.6:42.4	15.2	-5.9 ((*S*)-**4a**)
4	(*S*)-**6b**	52.8:47.2	5.6	-1.8 ((*S*)-**6a**)
5	(*S*)-**7b**	31.0:69.0	-38.0	+20.4 ((*S*)-**7a**)
6	(*S*)-**8b**	22.7:77.3	-54.6	+22.2 ((*S*)-**8a**)

[a] Excess of *M* conformer (%) = ([*M*]–[*P*])/([*M*]+[*P*])x100, where [*M*] and [*P*] are the amounts of *M* and *P* conformers calculated by B3LYP/6-31G*. [b] A_{CD} value: $A_{CD} = \Delta\varepsilon_1 - \Delta\varepsilon_2$, where $\Delta\varepsilon_1$ and $\Delta\varepsilon_2$ are intensities of first and second Cotton effects, respectively.

Theoretical calculations at HF/6-31G* level

Table S9. Calculated conformers of (*S*)-**2b** at HF/6-31G* level.

Entry	Conformer	Dihedral angle[a]	Δ*E*, kcal/mol	*K*[b]	Population, %
1	#M1	-44.26	0.00	1.00	67.8
2	#P1	45.25	0.43	0.47	32.2

[a] Dihedral angle of C6-C1-C1'-C6'. [b] Equilibrium constant at 293 K.

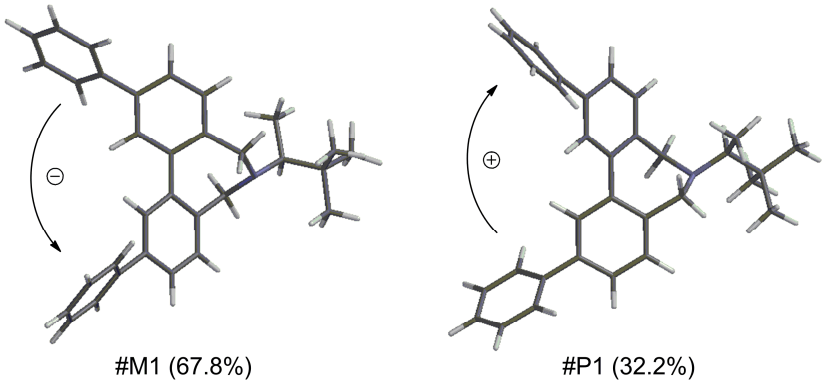

Figure S38. Two major conformers of (*S*)-**2b** at HF/6-31G* level.

Table S10. Calculated conformers of (*S*)-**3b** at HF/6-31G* level.

Entry	Conformer	Dihedral angle[a]	Δ*E*, kcal/mol	*K*[b]	Population, %
1	#M1	-44.47	0.00	1.00	54.8
2	#P1	44.69	0.22	0.69	37.6
3	#M7	-44.34	1.86	0.04	2.2
4	#P3	44.78	2.15	0.02	1.4
5	#P20	45.23	2.16	0.02	1.3
6	#M18	-44.46	2.40	0.02	0.9
7	#P5	44.61	2.61	0.01	0.6
8	#M5	-44.14	2.66	0.01	0.6
9	#P9	45.27	2.96	0.01	0.3
10	#M9	-44.27	2.98	0.01	0.3

[a] Dihedral angle of C6-C1-C1'-C6'. [b] Equilibrium constant at 293 K.

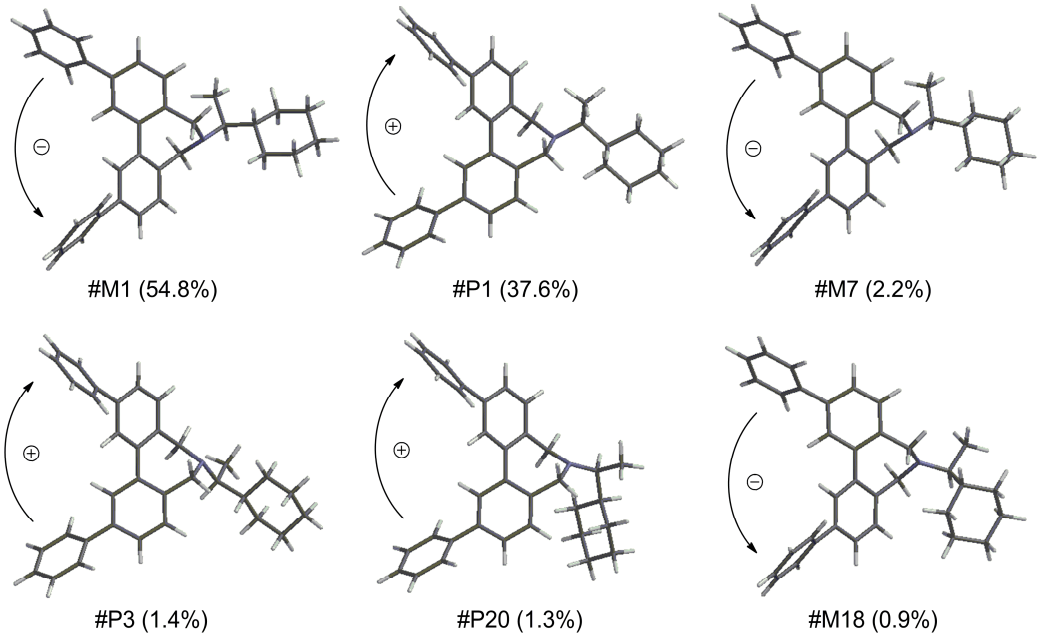

Figure S39. Six major conformers of (*S*)-**3b** at HF/6-31G* level.

Table S11. Calculated conformers of (*S*)-**4b** at HF/6-31G* level.

Entry	Conformer	Dihedral angle[a]	Δ*E*, kcal/mol	*K*[b]	Population, %
1	#M1	-44.48	0.00	1.00	54.9
2	#P1	44.70	0.23	0.68	37.2
3	#M5	-44.37	1.76	0.05	2.7
4	#P3	44.80	1.94	0.04	2.0
5	#P5	45.24	2.08	0.03	1.5
6	#M3	-44.16	2.40	0.02	0.9
7	#M7	-44.29	2.80	0.01	0.4
8	#P7	45.21	2.92	0.01	0.4

[a] Dihedral angle of C6-C1-C1'-C6'. [b] Equilibrium constant at 293 K.

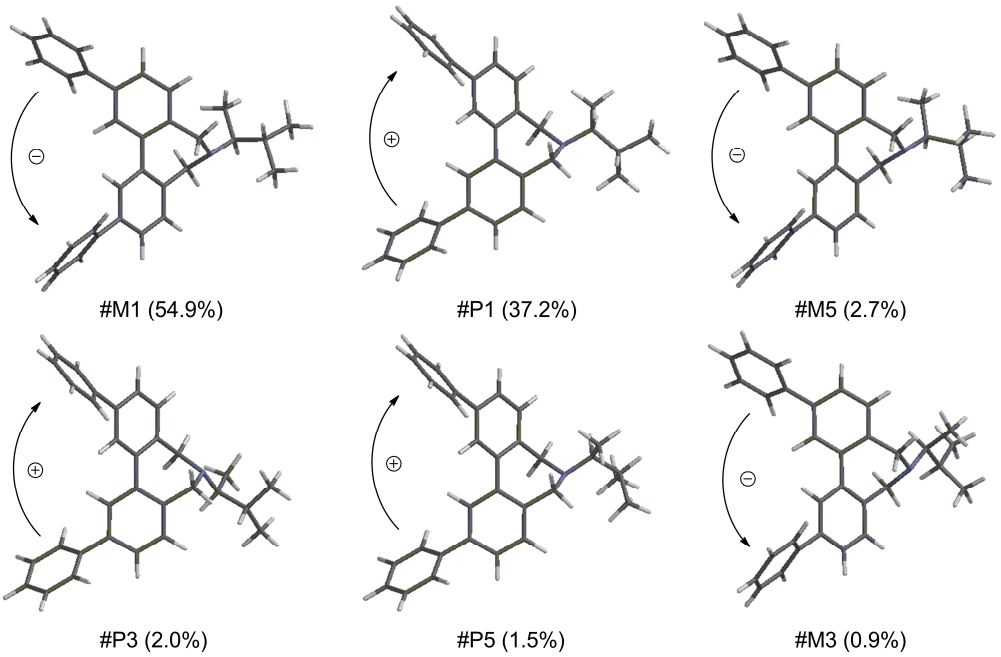

Figure S40. Six major conformers of (*S*)-**4b** at HF/6-31G* level.

Table S12. Calculated conformers of (*S*)-**6b** at HF/6-31G* level.

Entry	Conformer	Dihedral angle[a]	Δ*E*, kcal/mol	*K*[b]	Population, %
1	#M1	-44.48	0.00	1.00	40.9
2	#P1	44.69	0.17	0.75	30.8
3	#M5	-44.45	0.97	0.19	7.7
4	#P5	44.52	1.04	0.17	6.9
5	#P7	44.57	1.21	0.13	5.1
6	#M7	-44.54	1.31	0.11	4.3
7	#P3	44.42	1.96	0.03	1.4
8	#M3	-44.36	1.99	0.03	1.3
9	#P11	44.95	2.36	0.02	0.7
10	#P9	44.70	2.50	0.01	0.6
11	#M11	-44.68	2.91	0.01	0.3

[a] Dihedral angle of C6-C1-C1'-C6'. [b] Equilibrium constant at 293 K.

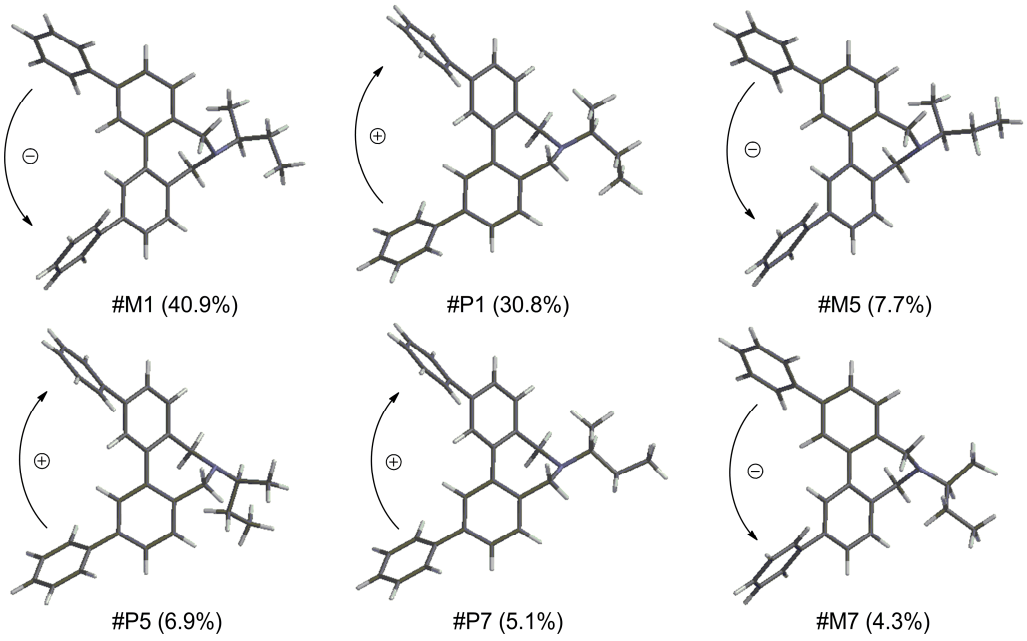

Figure S41. Six major conformers of (*S*)-**6b** at HF/6-31G* level.

Table S13. Calculated conformers of (*S*)-**7b** at HF/6-31G* level.

Entry	Conformer	Dihedral angle[a]	ΔE, kcal/mol	K[b]	Population, %
1	#P1	44.59	0.00	1.00	78.6
2	#M1	-44.58	0.92	0.21	16.3
3	#M5	-44.69	1.93	0.04	2.8
4	#P3	44.72	2.07	0.03	2.2

[a] Dihedral angle of C6-C1-C1'-C6'. [b] Equilibrium constant at 293 K.

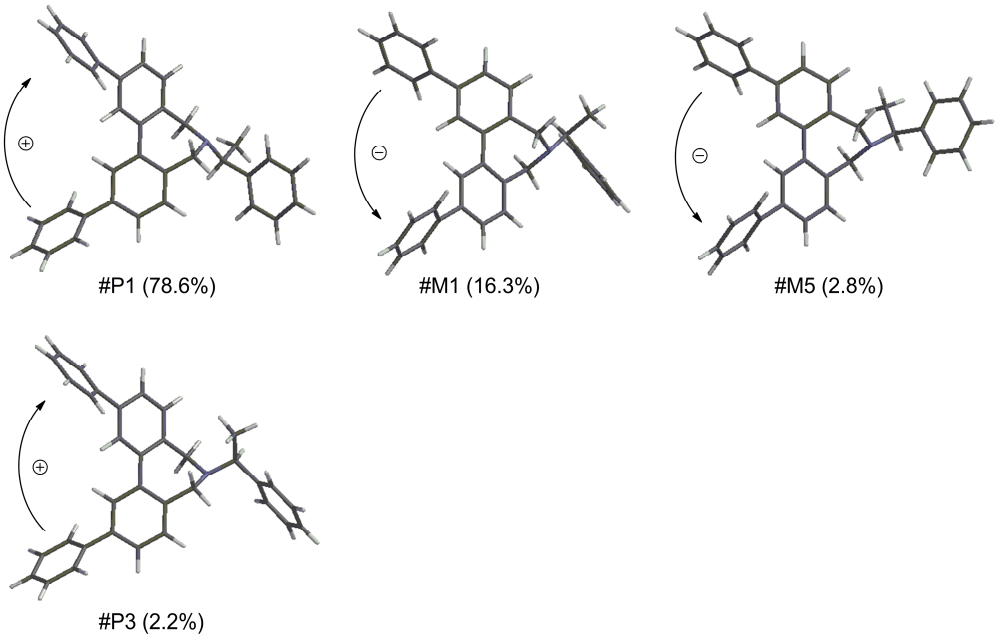

Figure S42. Four major conformers of (*S*)-**7b** at HF/6-31G* level.

Table S14. Calculated conformers of (*S*)-**8b** at HF/6-31G* level.

Entry	Conformer	Dihedral angle[a]	ΔE, kcal/mol	K[b]	Population, %
1	#P1	44.70	0.00	1.00	41.8
2	#P3	44.52	0.10	0.84	35.1
3	#M3	-44.64	0.83	0.24	10.0
4	#M1	-44.55	1.22	0.12	5.2
5	#M7	-44.65	1.34	0.10	4.2
6	#P5	44.60	1.40	0.09	3.8

[a] Dihedral angle of C6-C1-C1'-C6'. [b] Equilibrium constant at 293 K.

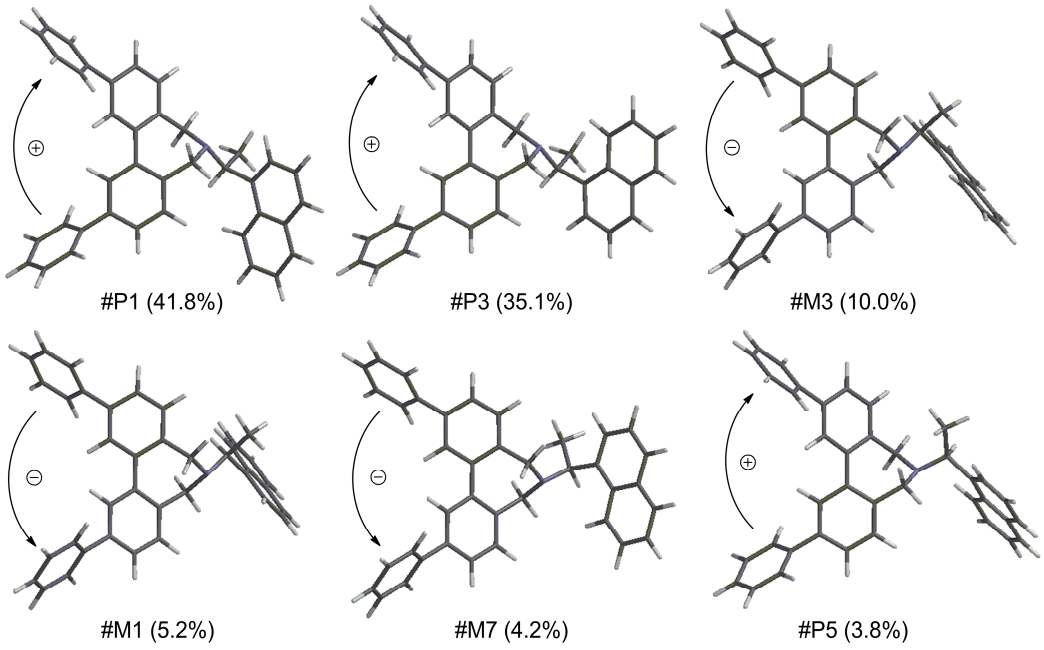

Figure S43. Six major conformers of (*S*)-**8b** at HF/6-31G* level.

Table S15. Comparison of the excess of *M* conformer and observed CD amplitude at HF/6-31G* level.

Entry	Compound	Calcurated ratio (*M*/*P*)	Excess of *M* confomer, %[a]	Observed CD amplitude (A_{CD} value)[b]
1	(*S*)-**2b**	67.8:32.2	35.6	–17.7 ((*S*)-**2a**)
2	(*S*)-**3b**	58.8:41.2	17.6	–7.5 ((*S*)-**3a**)
3	(*S*)-**4b**	58.9:41.1	17.8	–5.9 ((*S*)-**4a**)
4	(*S*)-**6b**	54.5:45.5	9.0	–1.8 ((*S*)-**6a**)
5	(*S*)-**7b**	19.1:80.9	–61.8	+20.4 ((*S*)-**7a**)
6	(*S*)-**8b**	19.3:80.7	–61.4	+22.2 ((*S*)-**8a**)

[a] Excess of *M* conformer (%) = ([*M*]–[*P*])/([*M*]+[*P*])x100, where [*M*] and [*P*] are the amounts of *M* and *P* conformers calculated by HF/6-31G*. [b] A_{CD} value: $A_{CD} = \Delta\varepsilon_1 - \Delta\varepsilon_2$, where $\Delta\varepsilon_1$ and $\Delta\varepsilon_2$ are intensities of first and second Cotton effects, respectively.

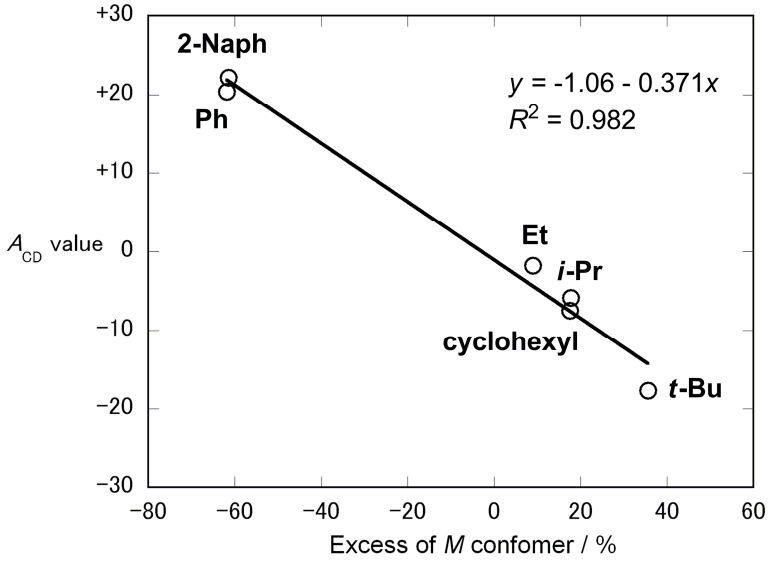

Figure S44. The relationship between the A_{CD} values and excess of *M* conformer. Excess of *M* conformer (%) = ([*M*]–[*P*])/([*M*]+[*P*])x100, where [*M*] and [*P*] are the amounts of *M* and *P* conformers calculated by HF/6-31G*, respectively.

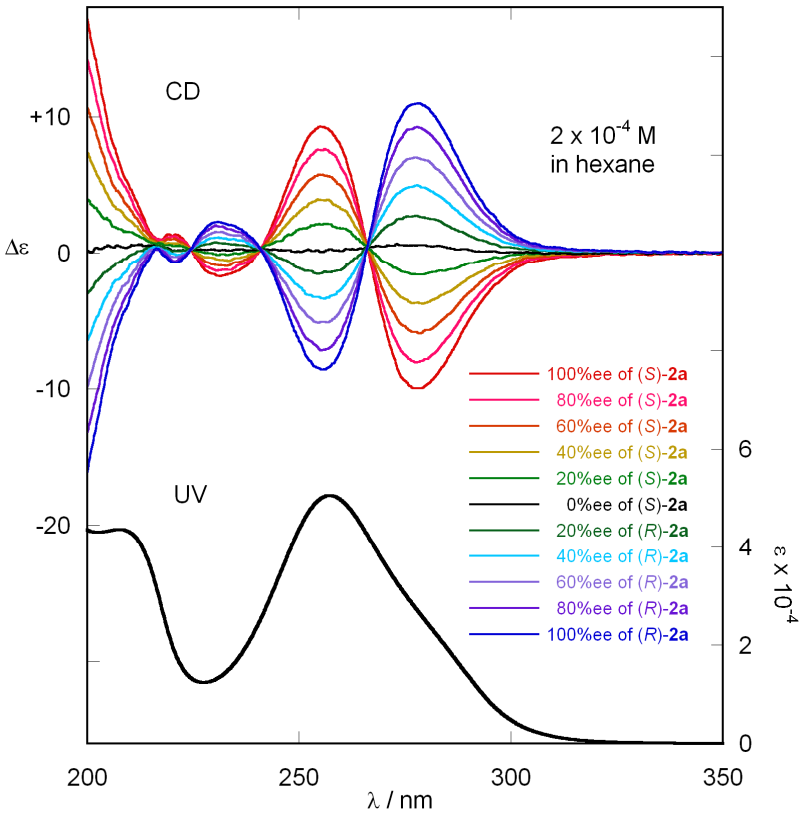

Figure S45. CD and UV Spectra of (*S*)-**2a** and (*R*)-**2a** with varying %ee value (2 x 10^{-4} M in hexane, 293 K).

X-ray Structure Determination

Crystals of (*S*)-**2a**, (*S*)-**3a**, and (*S*)-**6a** was mounted on the top of a glass fiber, and the data collection was carried out on a Bruker SMART diffractometer equipped with a CCD area detector at 100–120 K. The data were corrected for Lorentz and polarization effects, and absorption corrections were applied with the *SADABS* probram.[3] The structure was solved by direct methods and subsequent difference Fourier syntheses using the program *SHELXTL*.[4] All non-H atoms were refined anisotropically, and H atoms were placed in calculated positions and thereafter refined with U_{iso}(H) = 1.2U_{eq}(C).

Table S16. Crystal data and structure refinement for (*S*)-**2a**

Empirical formula	C34 H37 N O2	
Formula weight	491.65	
Temperature	120 K	
Wavelength	0.71073 Å	
Crystal system	Orthorhombic	
Space group	*P*2(1)2(1)2(1)	
Unit cell dimensions	a = 6.2995(3) Å	α = 90°.
	b = 20.1090(11) Å	β = 90°.
	c = 21.2319(12) Å	γ = 90°.
Volume	2689.6(2) Å^3	
Z	4	
Density (calculated)	1.214 Mg/m^3	
Absorption coefficient	0.074 mm^{-1}	
F(000)	1056	
Crystal size	0.38 x 0.23 x 0.14 mm^3	
Theta range for data collection	1.92 to 28.30°.	
Index ranges	–8<=h<=8, –26<=k<=26, –28<=l<=24	
Reflections collected	20137	
Independent reflections	6678 [R(int) = 0.0275]	
Completeness to theta = 28.30°	99.9 %	
Absorption correction	Empirical	
Max. and min. transmission	0.9901 and 0.9726	
Refinement method	Full-matrix least-squares on F^2	
Data / restraints / parameters	6678 / 0 / 482	
Goodness-of-fit on F^2	1.035	
Final R indices [I>2sigma(I)]	R_1 = 0.0442, wR_2 = 0.1016	
R indices (all data)	R_1 = 0.0489, wR_2 = 0.1043	
Absolute structure parameter	0.4(11)	
Largest diff. peak and hole	0.294 and –0.164 e.Å^{-3}	

Table S17. Crystal data and structure refinement for (*S*)-**3a**

Empirical formula	C36 H39 N O2	
Formula weight	517.68	
Temperature	100 K	
Wavelength	0.71073 Å	
Crystal system	Monoclinic	
Space group	*P*2(1)	
Unit cell dimensions	a = 5.8922(2) Å	α = 90°.
	b = 22.0263(9) Å	β = 96.6290(10)°.
	c = 11.1024(4) Å	γ = 90°.
Volume	1431.27(9) Å^3	
Z	2	
Density (calculated)	1.201 Mg/m^3	
Absorption coefficient	0.073 mm^{-1}	
F(000)	556	
Crystal size	0.24 x 0.17 x 0.13 mm^3	
Theta range for data collection	1.85 to 30.98°.	
Index ranges	–8<=h<=8, –16<=k<=31, –14<=l<=15	
Reflections collected	10826	
Independent reflections	5823 [R(int) = 0.0198]	
Completeness to theta = 30.98°	99.9 %	
Absorption correction	Empirical	
Max. and min. transmission	0.9905 and 0.9826	
Refinement method	Full-matrix least-squares on F^2	
Data / restraints / parameters	5823 / 1 / 508	
Goodness-of-fit on F^2	1.034	
Final R indices [I>2sigma(I)]	R_1 = 0.0386, wR_2 = 0.0934	
R indices (all data)	R_1 = 0.0457, wR_2 = 0.0981	
Absolute structure parameter	1.3(11)	
Largest diff. peak and hole	0.292 and –0.201 e.Å^{-3}	

Table S18. Crystal data and structure refinement for (*S*)-**6a**

Empirical formula	C32 H33 N O2	
Formula weight	463.59	
Temperature	100 K	
Wavelength	0.71073 Å	
Crystal system	Monoclinic	
Space group	*P*2(1)	
Unit cell dimensions	a = 8.5443(7) Å	α = 90°.
	b = 25.924(2) Å	β = 96.6650(10)°.
	c = 11.1528(9) Å	γ = 90°.
Volume	2453.7(3) Å^3	
Z	4	
Density (calculated)	1.255 Mg/m^3	
Absorption coefficient	0.077 mm^{-1}	
F(000)	992	
Crystal size	0.24 x 0.13 x 0.06 mm^3	
Theta range for data collection	1.84 to 26.45°.	
Index ranges	–10<=h<=7, –32<=k<=32, –13<=l<=13	
Reflections collected	14632	
Independent reflections	9414 [R(int) = 0.0358]	
Completeness to theta = 26.45°	99.8 %	
Absorption correction	Empirical	
Max. and min. transmission	0.9952 and 0.9819	
Refinement method	Full-matrix least-squares on F^2	
Data / restraints / parameters	9414 / 1 / 639	
Goodness-of-fit on F^2	1.019	
Final R indices [I>2sigma(I)]	R_1 = 0.0519, wR_2 = 0.0993	
R indices (all data)	R_1 = 0.0773, wR_2 = 0.1118	
Absolute structure parameter	1.0(14)	
Largest diff. peak and hole	0.220 and –0.211 e.Å^{-3}	

References

(1) Scheuermann, G. M.; Rumi, L.; Steurer, P.; Bannwarth, W.; Mulhaupt, R. *J. Am. Chem. Soc.* **2009**, *131*, 8262.

(2) Ooi, T.; Uematsu, Y.; Kameda, M.; Maruoka, K. Tetrahedron **2006**, *62*, 11425.

(3) Sheldrick, G. M. *Program for absorption correction of area detector frames*; Bruker AXS, Inc.: Madison, WI, 1996.

(4) *SHELXTL*, *version 5.1*; Bruker AXS, Inc.: Madison, WI, 1997.